

65



68 Estimates based on model simulations have suggested that ClNO₂ provides a source of Cl atoms totaling
69 0.66 Tg Cl a⁻¹, with the vast majority (95%) being in the Northern Hemisphere (Sherwen et al., 2016).
70 The relative contribution of ClNO₂ to global tropospheric Cl atoms is 14% on average and exhibits clear
71 regional variations (Sherwen et al., 2016). For example, the study by Riedel et al. (2012) reported that
72 the relative contribution is approximately 45% in Los Angeles based on a simple box model combined
73 with local observations.

74 The heterogeneous formation of ClNO₂ also serves as a reservoir for reactive nitrogen at night. The rapid
75 photolysis of ClNO₂ at daytime (R4) not only releases highly reactive Cl atom but also recycles NO₂ back
76 to the atmosphere, which as well significantly affect the daytime photochemistry (Riedel et al., 2014). ~~It~~
77 ~~was suggested~~ Previous studies global and hemispheric models found that the heterogeneous reaction
78 ~~between~~ N₂O₅ + Cl chemistry and chloride-containing aerosol could increase monthly mean values of
79 the maximum daily 8h average (MDA8) O₃ concentrations by 1.0 – 8.0 ppbv in most Northern
80 Hemisphere regions (Sarwar et al., 2014; Wang et al., 2019). The reaction also impacts secondary aerosol
81 formation, mainly through the recycling of NO_x (Staudt et al., 2019; Mitroo et al., 2019). For example,
82 Sarwar et al. (2014) estimated that ClNO₂ production decreases nitrate by 3.3% in winter and 0.3% in
83 summer averaged over the entire Northern Hemisphere. The influence of the heterogeneous formation of
84 ClNO₂ in China is even larger due to the polluted environment, leading to an increase in ozone
85 concentrations by up to 7 ppbv, and a decrease in total nitrate by up to 2.35 μg m⁻³ on monthly mean
86 basis (Li et al., 2016; Sarwar et al., 2014)

87 ~~There are two key parameters determining the heterogeneous uptake of N₂O₅, including the uptake~~
88 ~~coefficient of N₂O₅ (γ_{N₂O₅}) and the ClNO₂ yield (φ_{ClNO₂}). There are two key parameters that determine~~
89 ~~the uptake efficiency of N₂O₅ and production of ClNO₂, the aerosol uptake coefficient of N₂O₅ (γ_{N₂O₅})~~
90 ~~and the ClNO₂ yield (φ_{ClNO₂}). The most widely used parameterization for γ_{N₂O₅} and φ_{ClNO₂} was proposed~~

带格式的：下标

91 by Bertram and Thornton (2009) (hereinafter referred to as hereafter BT09), which is based on the
92 laboratory studies with considerations of ~~temperature, relative humidity (RH), aerosol water content,~~
93 concentrations of nitrate and chloride, and specific surface area (i.e. the ratio of surface area
94 ~~concentrations to total particle volume concentrations to surface area concentration~~). However, recent
95 field and model studies have shown that this parameterization would overestimate both $\gamma_{\text{N}_2\text{O}_5}$ and ϕ_{ClNO_2} ,
96 especially in regions with high Cl levels (Mcduffie et al., 2018b; Mcduffie et al., 2018a; Xia et al., 2019;
97 Chang et al., 2016; Hong et al., 2020; Yu et al., 2020). The discrepancies could be partly attributed to the
98 complexity of atmospheric aerosols (e.g. mixing state and complex coating materials) in contrast to the
99 simple proxies used in laboratory studies (Yu et al., 2020). ~~For example, the overestimation~~ Specifically,
100 ~~the suppressive effect of organic coatings is not considered in- of $\gamma_{\text{N}_2\text{O}_5}$ from- BT09- could be partly~~
101 ~~explained that they did not consider the suppression of organic aerosol. Specifically, the presence of~~
102 ~~organic aerosol that may reduce the uptake of N_2O_5 is not considered in $\gamma_{\text{N}_2\text{O}_5}$ from Bertram and~~
103 ~~Thornton (2009).~~ Several parameterizations updated from ~~the one by Bertram and Thornton (20BT0909)~~
104 have been proposed by more recent studies based on field measurements and box model studies (Yu et
105 al., 2020; Mcduffie et al., 2018a; Mcduffie et al., 2018b; Xia et al., 2019). However, a full evaluation of
106 ~~the representativeness of different parameterizations for the N_2O_5 - ClNO_2 chemistry and the associated~~
107 ~~impacts on ambient air quality is not available yet.~~ However, ~~thesome of these previous field-based~~
108 ~~parameterizations were derived from different observations under different ambient conditions which~~
109 ~~may not be applicable to the highly polluted regions in China. A full evaluation of the representativeness~~
110 ~~of different parameterizations for the heterogeneous N_2O_5 + Cl chemistry under different conditions in~~
111 ~~China and the associated impacts on ambient air quality in China is not available yet.~~

112 In addition to the parameterization, the influence of the ~~heterogeneous N_2O_5 + Cl chemistry~~ N_2O_5 -
113 ~~ClNO_2 chemistry~~ is also sensitive to chlorine emissions. In early modelling studies, global tropospheric
114 chlorine is mainly from sea salt aerosols (SSA), and most of the chlorine over continental regions in
115 North America and Europe is dominated by the long-range transport of SSA (Wang et al., 2019; Sherwen
116 et al., 2017). ~~The study by Wang et al. (2019) found an addition of anthropogenic chlorine emissions in~~
117 ~~the model would result in overestimates of HCl observations in the U.S and suggested insignificant~~
118 ~~influence of anthropogenic Cl in the U.S. However, there are also studies pointing out the~~
119 ~~importance of anthropogenic chlorine emissions in China (Le Breton et al., 2018; Yang et al., 2018;~~

带格式的：下标

带格式的：下标

带格式的：字体：非倾斜

120 [Hong et al., 2020](#))~~ref~~. ~~The importance of anthropogenic chlorine emissions, which were ignored in~~
121 ~~most studies, has been raised recently based on both field measurements and model simulations (Le~~
122 ~~Breton et al., 2018; Yang et al., 2018; Wang et al., 2020b; Hong et al., 2020).~~The study by Wang et al.
123 (2020b) ~~suggested that anthropogenic chlorine from anthropogenic emissions in China is~~are more than
124 ~~8 times higher than that those in the U.S. on annual average suggested and that anthropogenic~~
125 ~~emissions~~and could dominate reactive chlorine in China, resulting in an increase in PM_{2.5} and Ozone by
126 up to 3.2 μg m⁻³ and 1.9 ppbv on annual mean basis, respectively. The comprehensive effects of
127 anthropogenic chlorine on air quality as well as their sensitivities to different parameterizations for [the](#)
128 [heterogeneous](#) N₂O₅ ~~±~~ CINO₂ chemistry, however, has not been investigated in previous studies.

129 In this work, we use the GEOS-Chem model to investigate the impacts of chlorine chemistry including
130 the heterogeneous N₂O₅ ~~±~~ CINO₂ chemistry on air quality in China. Multiple observational data sets,
131 including N₂O₅, CINO₂, O₃, PM_{2.5} and its chemical ~~speeies~~compositions from different representative
132 sites across China, are used to assess the model performance. With comprehensive chlorine emissions as
133 well as appropriate parameterizations for [the heterogeneous](#) N₂O₅ ~~±~~ CINO₂ chemistry, our objectives
134 are: 1) to improve the model's performance regarding the simulation of particulate chloride, CINO₂,
135 N₂O₅, PM_{2.5} and O₃ concentrations; and 2) to extend the investigation on the effects of chlorine chemistry
136 on both PM_{2.5} and ozone pollution in China as well as their sensitivities to anthropogenic chlorine
137 emissions and the parameterizations for [the heterogeneous](#) N₂O₅ ~~±~~ CINO₂ chemistry.

138 2 Methodology

139 2.1 GEOS-Chem Model

140 The GEOS-Chem model (version 12.9.3, <http://www.geos-chem.org>, DOI: 10.5281/zenodo.3974569) is
141 driven by assimilated meteorological fields GEOS-FP from the NASA Global Modeling and Assimilation
142 Office (GMAO) at NASA Goddard Space Flight Center. The simulation in this study was conducted in
143 a nested-grid model with a native horizontal resolution of 0.25° × 0.3125° (latitude × longitude) and 47
144 vertical levels over East Asia (70° – 140° E, 15° S – 55° N). The dynamical boundary conditions were
145 from a global simulation with a horizontal resolution of 2° × 2.5°. We initialized the model with a 1-month

146 spin up followed by a 1-year simulation for 2018. The simulation included a detailed representation of
147 coupled NO_x – ozone – VOCs – aerosol – halogen chemistry (Sherwen et al., 2016; Wang et al., 2019).
148 Previous studies have demonstrated the ability of GEOS-Chem to reasonably reproduce the magnitude
149 and seasonal variation of surface ozone and particulate matter over East Asia and China (Wang et al.,
150 2013; Geng et al., 2015; Li et al., 2019).

151 2.1.1 Chlorine Chemistry

152 The GEOS-Chem model includes a comprehensive chlorine chemistry mechanism coupled with bromine
153 and iodine chemistry. Full details could be found in the study of (Wang et al., (2019) ~~Wang et al. (2019b)~~).
154 Briefly, the model includes 12 gas-phase inorganic chlorine species (Cl, Cl₂, Cl₂O₂, ClNO₂, ClNO₃, ClO,
155 ClOO, OClO, BrCl, ICl, HOCl, HCl), 3 gas-phase organic chlorine (CH₃Cl, CH₂Cl₂, CHCl₃), and aerosol
156 Cl⁻ in two size bins (fine mode with radius ≤ 0.5 μm and coarse mode with radius > 0.5 μm). The gas-
157 aerosol equilibrium between HCl and Cl⁻ is calculated with ISORROPIA II (Fountoukis and Nenes, 2007)
158 as part of the H₂SO₄ – HCl – HNO₃ – NH₃ – non-volatile cations (NVCs) thermodynamic system, where
159 Na⁺ is used as a proxy for NVCs.

160 The heterogeneous uptake of N₂O₅ on aerosol surfaces leading to the production of ClNO₂ and HNO₃
161 has also been included in GEOS-Chem with the parameterizations for γ_{N₂O₅} and φ_{ClNO₂} proposed by
162 McDuffie et al. (2018b; 2018a) by default (hereinafter referred to as McDuffie pParameterization).
163 McDuffie parameterization is the first field-based empirical parameterization derived from the
164 framework proposed in multiple laboratory studies including BT09 (Anttila et al., 2006; Bertram and
165 Thomton, 2009; Riemer et al., 2009) to account for the uptake dependence on aerosol water and nitrate
166 concentrations as well as the resistance from an organic coating. The coefficients for McDuffie
167 parameterization were derived from applying a box model to observations of N₂O₅, ClNO₂, O₃, and NO_x
168 mixing ratios during the winter in the eastern U.S.-. The parameterization for γ_{N₂O₅} accounts for the N₂O₅
169 uptake on the inorganic aerosol core coating with an organic shell both the inorganic and organic aerosol
170 components and, The γ_{N₂O₅} which can be described by Eq. 1 – 3:

$$\frac{1}{\gamma_{N_2O_5}} = \frac{1}{\gamma_{core}} + \frac{1}{\gamma_{coat}} \quad \text{Eq. 1}$$

带格式的：字体：非倾斜

带格式的：字体：非倾斜

带格式的：字体：非倾斜

带格式的：字体：倾斜

带格式的：下标

带格式的：下标

$$\gamma_{\text{core}} = \frac{4V}{c \cdot S_a} K_H \times 2.14 \times 10^5 \times [\text{H}_2\text{O}] k_{\text{RR}} \left(1 - \frac{1}{\left(\frac{k_{\text{H}_2\text{O}}}{k_{\text{NO}_3^-}} \frac{[\text{H}_2\text{O}]}{[\text{NO}_3^-]} + 1 \right)} \right) \quad \text{Eq.2}$$

带格式的

$$\gamma_{\text{coat}} = \frac{4RT\varepsilon H_{\text{aq}} D_{\text{aq}} R_c}{c l R_p} \quad \text{Eq.3}$$

带格式的：两端对齐

Where γ_{core} represents the reactive uptake of inorganic aerosol core, and γ_{coat} represents the retardation of the organic coating.

带格式的

$$\gamma_{\text{coat}} = \frac{4RT\varepsilon H_{\text{aq}} D_{\text{aq}} R_c}{c l R_p} \quad \text{Eq.3}$$

带格式的

Where γ_{core} represents the reactive uptake of inorganic aerosol core; and γ_{coat} represents the retardation of the organic coating; c is the average gas-phase thermal velocity of N_2O_5 (m s^{-1}), V is the total particle volume concentration ($\text{m}^3 \text{m}^{-3}$), S_a is the total particle surface area concentration ($\text{m}^2 \text{m}^{-3}$), K_H is the unitless Henry's law coefficient for N_2O_5 with a constant value of 51, $[\text{H}_2\text{O}]$ and $[\text{NO}_3^-]$ are the concentrations of aerosol liquid water content and aerosol nitrate (mol L^{-1}), respectively, k_{RR} is a linear function of water ($= 2.14 \times 10^5 \times [\text{H}_2\text{O}] (\text{M}^{-1} \text{s}^{-1})$), and $k_{\text{H}_2\text{O}}/k_{\text{NO}_3^-}$ is represents the rate constant ratio representing the competing competition between aerosol-phase H_2O and NO_3^- for the $\text{H}_2\text{ONO}_2^+(\text{aq})$ reactions of intermediate $\text{H}_2\text{ONO}_2^+(\text{aq})$ with H_2O over NO_3^- and at 0.04 in Eq.2 represent the relative rates of competing reactions of intermediate $\text{H}_2\text{ONO}_2^+(\text{aq})$ with H_2O over NO_3^- ($= 0.04$); R is the ideal gas constant, T is the temperature (K), H_{aq} and D_{aq} are the aqueous Henry's law constant and aqueous-phase diffusion coefficient of N_2O_5 , respectively, ε is a scaling coefficient, which increases linearly a linear combination with the increase of relative humidity (RH) and O:C ratio ($= 0.15 \times \text{O:C} + 0.0016 \times \text{RH}$), and R_p and R_c , R_c , and l are the total particle radius, inorganic core radius and organic coating thickness, respectively (m), radii of the inorganic core and the whole particle with organic coating (m), l is the thickness of organic coating (m). More details of the parameterization can be referred to McDuffie et al. (2018b).

带格式的

ϕ_{ClNO_2} is calculated following the study of Bertram and Thornton (2009) BT09, but is reduced by 75% based on the observations conducted in eastern U.S. and offshore in spring 2015 (i.e. the WINTER aircraft campaign) (McDuffie et al., 2018b) (Lee et al., 2018). It could be described by Eq. 24:

带格式的：段落间距段后：1 行

$$\phi_{\text{ClNO}_2} = 0.25 \times \left(k_c \frac{k_{\text{Cl}^-} [\text{H}_2\text{O}]}{k_{\text{Cl}^-} [\text{Cl}^-]} + 1 \right)^{-1} \quad \text{Eq. 24}$$

批注 [MOU1]: 没按 review 改

199 Where $[H_2O]$ and $[Cl^-]$ are the concentrations of aerosol liquid water content and aerosol chloride (mol
 200 L^{-1}), respectively, and k_2/k_3 is the rate constant ratio representing the competition between aerosol-
 201 phase H_2O and Cl^- for the $H_2ONO_2^+$ (aq) intermediate and is fixed at represents the relative rates of
 202 competing reactions of intermediate $H_2ONO_2^+$ (aq) with H_2O over Cl^- (=1/450 here, and). $[Cl^-]$ is the
 203 concentration of aerosol chloride (mol L^{-1}). For more detailed description of McDuffie parameterization,
 204 readers are referred to McDuffie et al. (2018b; 2018a). Keep it in mind that the coefficients for the
 205 parameterizations in Eq. 1–4 were derived to better reproduce wintertime observations in the eastern
 206 U.S. However, there are large uncertainties in both the values of the coefficients and functional form of
 207 the parameterizations, specifically related to their applicability to other regions. The McDuffie
 208 parameterization can reproduce observed mean values of $\gamma_{N_2O_5}$ and ϕ_{ClNO_2} in eastern U.S. (Meduffie et
 209 al., 2018b; Meduffie et al., 2018a), but is still of great uncertainty. However, there still exist large
 210 uncertainties in both the values of the coefficients and functional form of the parameterizations,
 211 specifically related to their applicability to other regions.

212 Recently, Yu et al. (2020) proposed new parameterizations of $\gamma_{N_2O_5}$ and ϕ_{ClNO_2} based on BT09 to account
 213 for the dependence on aerosol water, nitrate, and chloride concentrations but with coefficients derived
 214 from uptake coefficients directly measured on ambient aerosol in two rural sites in China the direct
 215 measurements at two sites in northern and southern China representing different atmospheric conditions.
 216 The parameterizations (hereinafter referred to as Yu parameterization) of $\gamma_{N_2O_5}$ and ϕ_{ClNO_2} (hereinafter
 217 referred to as Yu parameterization) are described by Eq. 3–4–5–6, respectively:

$$218 \gamma_{N_2O_5} = \frac{4V}{c \cdot S_a} K_H \times 3.0 \times 10^4 \times [H_2O]^{6.12} \times 10^6 \times \frac{[H_2O]^{1/2}}{e \cdot S_a} \left(1 - \frac{1}{k_a \frac{[H_2O]}{[NO_3^-]} + k_b \frac{[Cl^-]}{[NO_3^-]} + 1} \right) \quad \text{Eq. 35}$$

$$221 \phi_{ClNO_2} = \left(1 + k_c \frac{k_{\text{eq}}[H_2O]}{k_{\text{eq}}[Cl^-]} \right)^{-1} \quad \text{Eq. 46}$$

222 Where c is the average gas phase thermal velocity of N_2O_5 ($m \cdot s^{-1}$), V is the total particle volume
 223 concentration ($m^3 \cdot m^{-3}$), S_a is the total particle surface area concentration ($m^2 \cdot m^{-3}$), K_H is the unitless
 224 Henry's law coefficient for N_2O_5 with a constant value of 51, $[H_2O]$, $[NO_3^-]$ and $[Cl^-]$ are the
 225 concentrations of aerosol liquid water content, aerosol nitrate and aerosol chloride (mol L^{-1}), respectively,

带格式的：上标

带格式的：字体：非倾斜

带格式的：字体：非倾斜

带格式的：字体：非倾斜

带格式的：字体：非倾斜

带格式的：字体：非倾斜

带格式的：非上标/下标

带格式的：左，段落间距段后：1行

带格式的：上标

226 k_c represents the relative rates of competing reactions of intermediate H_2ONO_2^+ (aq) with H_2O over NO_3^-
 227 ($=0.033$), k_0 is the rate constant ratio representing the competition between aerosol-phase Cl^- and NO_3^-
 228 for the H_2ONO_2^+ (aq) intermediate and is fixed at represents the relative rates of competing reactions of
 229 intermediate H_2ONO_2^+ (aq) with Cl^- over NO_3^- ($=3.4$). In contrast to McDuffie parameterization, k_a and
 230 k_c represents the relative rates of competing reactions of intermediate H_2ONO_2^+ in Yu parameterization
 231 (aq) with H_2O over Cl^- are fixed at 0.033 and \bar{v} ($=1/150$, respectively), all variables are same as Eq. 2 and
 232 Eq. 4 except $[\text{Cl}^-]$ is the concentrations of aerosol liquid water content and aerosol chloride (mol L^{-1}),
 233 $k_2/k_3 = 1/150$, respectively, v is an average gas phase thermal velocity of N_2O_5 , V and S_a are particle
 234 volume and surface area densities, respectively; $[\text{H}_2\text{O}]$, $[\text{Cl}^-]$ and $[\text{NO}_3^-]$ are the concentrations of aerosol
 235 liquid water content, aerosol chloride and aerosol nitrate, respectively.

带格式的：上标

带格式的：下标

236 Although both the two parameterizations are based on referred are developed based on BT09, to the
 237 study of Bertram and Thornton (2009),

238 here exist significant differences of $\gamma_{\text{N}_2\text{O}_5}$ and ρ_{ClNO_2} between the McDuffie and Yu parameterizations. In
 239 general, the McDuffie Parameterization is derived from parameterizations proposed in multiple
 240 laboratory studies (Anttila et al., 2006; Bertram and Thornton, 2009; Riemer et al., 2009), while the
 241 coefficients were derived by fitting a chemical box model to aircraft observations during the winter over
 242 the eastern U.S. The Yu Parameterization is mainly based on the study of Bertram and Thornton (2009),
 243 with coefficients derived from uptake coefficients directly measured on ambient aerosol in two rural sites
 244 in China. For $\gamma_{\text{N}_2\text{O}_5}$, the McDuffie parameterization generally follows the study of Bertram and Thornton
 245 (2009) BT09 for the calculation of the uptake on inorganic aerosols (i.e. γ_{core}), but excludes while exclude
 246 any the dependence on aerosol chloride because it could so as to better reproduce observed wintertime
 247 reactive nitrogen in the eastern U.S. On the other hand, moreover, the parameterization includes accounts
 248 for the suppressive effects of the organics (i.e. γ_{coat}) aerosol as a resistive coating, which is not directly
 249 included in BT09 (Anttila et al., 2006; Riemer et al., 2009; Morgan et al., 2015ref), as suggested by
 250 multiple laboratory studies (Anttila et al., 2006; Riemer et al., 2009; Morgan et al., 2015), important in
 251 the estimation of N_2O_5 uptake. Unlike in contrast to McDuffie parameterization, Yu parameterization
 252 Yu et al. (2020) suggested that excluding the organic suppression and but including the chloride
 253 enhancement could so as to better best-reproduce the observed $\gamma_{\text{N}_2\text{O}_5}$ observed in China (ref Yu et al., 2020).

带格式的：字体：倾斜

254 It is worth mentioning that the coefficients applied in the parameterization of $\gamma_{\text{N}_2\text{O}_5}$ also differ between
255 McDuffie and Yu parameterizations as both are fixed to reproduce the ambient observation representing
256 different pollution conditions. For example, k_a is equal to 0.04 in Eq. 2 but 0.033 in Eq. 5. The $\gamma_{\text{N}_2\text{O}_5}$ in
257 McDuffie parameterization is thus expected to be lower compared with the Yu parameterization due to
258 the resistance from organic coating and the lack of the chloride enhancement. For α_{ClNO_2} , both of the
259 McDuffie and Yu parameterizations are based on BT09 the study of Bertram and Thornton (2009), but,
260 while with different coefficients (i.e. $k_c/k_3 = 1/450$ in Eq. 44 and $1/150$ in Eq. Eq.66). Although k_c in Eq.
261 4 is relatively smaller, the scaling factor of 0.25 applied in Eq. 4 ultimately results in a much smaller
262 α_{ClNO_2} in McDuffie parameterization and scaling factors (0.25 in Eq.4) derived compared with Yu
263 parameterization under the same condition. Again, keep it in mind that McDuffie parameterization is
264 derived from fits to ~~from fits to observations~~ over the eastern U.S. (McDuffie et al., 2018a) while Yu
265 parameterization is fitted to observations at ~~and rural locations~~ in China (Yu et al., 2020), ~~respectively~~.

带格式的: 字体: 倾斜

带格式的: 非上标/ 下标

带格式的: 字体: 倾斜

266 In this study, we updated the parameterizations for $\gamma_{\text{N}_2\text{O}_5}$ and α_{ClNO_2} in the heterogeneous $\text{N}_2\text{O}_5 + \text{Cl}$
267 ~~heterogeneous chemistry~~ (hereinafter referred to as parameterizations for heterogeneous $\text{N}_2\text{O}_5 + \text{Cl}$
268 ~~chemistry~~) updated the $\text{N}_2\text{O}_5 - \text{ClNO}_2$ chemistry in the GEOS-Chem with the Yu parameterization.
269 Additional simulation cases were also performed to evaluate the representativeness of both the Yu and
270 McDuffie parameterizations regarding the simulation of N_2O_5 , ClNO_2 , O_3 , $\text{PM}_{2.5}$ and its chemical
271 composition ~~speciation~~ in China. Detailed description of the model setup for related cases is provided
272 below in Section 2.1.3.

带格式的: 下标

带格式的: 下标

带格式的: 下标

带格式的: 下标

273 2.1.2 Emissions

274 The study uses the Hemispheric Transport of Air Pollution (HTAPv2, <http://www.htap.org/>) based on the
275 emission of 2010 as a global anthropogenic inventory. This inventory is overwritten by a regional
276 emission inventory MIX (with a horizontal resolution of $0.25^\circ \times 0.25^\circ$) over East Asia based on the
277 emission in 2017, which is developed for the Model Inter-Comparison Study for Asia (MICS-Asia) and
278 covers all major anthropogenic sources in 30 Asian countries and regions (Li et al., 2017). In addition,
279 anthropogenic emissions of black carbon (BC) and organic carbon (OC) in Guangdong province, China
280 ($109^\circ - 117^\circ \text{ E}$, $20^\circ - 26^\circ \text{ N}$) are overwritten by a more recent high-resolution inventory ($9 \text{ km} \times 9 \text{ km}$)
281 described by Huang et al. (2021). Biomass burning emissions are from the Global Fire Emissions

282 Database (GFED4) (Van et al., 2010) with a 3-hour time resolution. And the biogenic emissions of VOCs
283 are calculated based on the Model of Emissions of Gases and Aerosols from Nature (MEGAN2.1)
284 (Guenther et al., 2006).

285 Table 1 lists Cl emissions from all sources in the model. The global tropospheric chlorine by default in
286 the model is mainly from the mobilization of Cl⁻ from SSA distributed over two size bins (fine and coarse
287 modes) (Wang et al., 2019), which is computed online as the integrals of the size-dependent source
288 function depending on wind speeds and sea surface temperatures (Jaeglé et al., 2011). During the
289 simulation year of 2018, SSA contributes 6.5×10^4 Gg Cl⁻, most of which however are distributed over
290 the ocean due to its relatively short lifetime (~1.5 days) (Choi et al., 2020). The release of atomic Cl
291 from organic chlorine (CH₃Cl, CH₂Cl₂ and CHCl₃) via the oxidation by OH and Cl is also included in
292 the model by default. These organic chlorine gases are mainly of biogenic marine origin (Simmonds et
293 al., 2006), with a mean tropospheric lifetime longer than 250 days (Wang et al., 2020b), and are simulated
294 in the model by imposing fixed surface concentrations as described by Schmidt et al. (2016). Total
295 emissions of Cl atom from CH₃Cl, CH₂Cl₂, and CHCl₃ are ~~estimated~~calculated to be 3.8, 2.4, and 0.70
296 Gg Cl a⁻¹, respectively.

297 Considering the importance of anthropogenic chlorine in China, we have further updated chlorine
298 inventories in the model to account for anthropogenic HCl, Cl₂ and fine particulate Cl⁻, as well as biomass
299 burning HCl and Cl⁻ emissions (also shown in Table 1 and S1). For fine particulate Cl⁻ from both
300 anthropogenic and biomass burning, the emissions are estimated based on PM_{2.5} emissions from MIX
301 and GFED4 inventories combined with the emission ratios of fine particulate Cl⁻ versus PM_{2.5} for
302 different emission sectors adopted from the study of Fu et al. (2018). Estimated Cl⁻ emissions from
303 anthropogenic and biomass burning are 379 and 120 Gg, respectively, comparable to the results of 486
304 Gg in total for the year of 2014 by Fu et al. (2018). The anthropogenic emissions of HCl and Cl₂ are from
305 ACEIC (Anthropogenic Chlorine Emissions Inventory for China) (Liu et al., 2018) and are estimated to
306 be 218 and 8.9 Gg Cl in China, respectively. For HCl from biomass burning, the emission factors from
307 Lobert et al. (1999) are used for different types of biomass provided in GFED4, and a total emission of
308 30 Gg Cl is obtained in China in 2018. Total implemented chlorine emission for the simulation year of
309 2018 is 756 Gg Cl (~~anthropogenic emissions of HCl, Cl₂, and Cl⁻ from different sectors are shown at~~

带格式的: 字体: 10 磅, 非加粗

带格式的: 字体: 10 磅, 非加粗, 上标

带格式的: 字体: 10 磅, 非加粗

带格式的：非突出显示

310 [Table S1](#)).

311 Figure 1 shows the distribution of Cl emissions from the sources mentioned above. Anthropogenic and
312 biomass burning emissions of HCl are concentrated in the Northeast Plain (~~NP~~), North China Plain (~~NCP~~),
313 Yangtze River Delta (~~YRD~~), and Sichuan Basin (~~SCB~~), and ~~could be~~ up to 320 kg Cl km⁻² a⁻¹ in the
314 ~~SCB~~ [Sichuan Basin](#). Emissions of HCl are low in South China, mainly due to the low chlorine content of
315 coal in these regions (Hong et al., 2020). The relative contribution of biomass burning to total HCl
316 emissions in China is 14% on average, but could become dominant in the [Northeast Plain](#) ~~NP~~ due to the
317 discrepancies in the spatial distributions of anthropogenic and biomass burning emissions. The
318 anthropogenic Cl₂ emissions have a similar spatial distribution to that of HCl, but are one order of
319 magnitude lower than HCl emissions. The distribution of non-sea salt Cl⁻ emissions is also similar to that
320 of HCl and Cl₂, except that non-sea salt Cl⁻ emissions are also high in Central China. In contrast,
321 emissions of sea salt Cl⁻ (Fig. S1) are mainly distributed over the ocean, implying limited influences over
322 inland due to rapid deposition during transport. The spatial distributions of different organic chlorine
323 sources are similar, with maximums (~ 0.5 kg Cl km⁻² a⁻¹) in coastal regions (Fig. S1).

324 2.1.3 Model setup for different simulation cases

325 In this study, we conducted a series of simulation cases to investigate the effects of chlorine chemistry
326 on air quality in China, the role of N₂O₅ – ClNO₂ chemistry, and the associated sensitivities to chlorine
327 emissions as well as the parameterizations for N₂O₅ – ClNO₂ chemistry. Detailed model setup for those
328 cases is listed in Table 2. The Base case is the one with all updates in this study, including additional
329 chlorine sources from anthropogenic and biomass burning emissions as well as [N₂O₅ uptake and ClNO₂](#)
330 ~~production~~ [improved N₂O₅ – ClNO₂ chemistry](#) represented by ~~the~~ Yu parameterization. The NoEm case
331 is conducted with a similar setup as the Base case but only includes chlorine emissions from SSA and
332 organic chlorine sources so as to evaluate the model improvement originated from the updated chlorine
333 emissions through the comparison with the Base case. The McDuffie case is also performed using the
334 McDuffie instead of Yu parameterization for $\gamma_{\text{N}_2\text{O}_5}$ and ϕ_{ClNO_2} while keeping others the same as the Base
335 case so as to evaluate the discrepancies originated from different parameterizations for the [heterogeneous](#)
336 [N₂O₅ + ClN₂O₅ – ClNO₂](#) chemistry.

337 In addition, while keeping others the same as the Base case, the NoHet case sets ϕ_{ClNO_2} to zero (Eq.6)
338 and removes the enhancement of N_2O_5 uptake from aerosol chloride (i.e. $[\text{Cl}^-] = 0$ in Eq. 5). The
339 comparison between the Base and NoHet cases could thus, but keeps others the same as the Base
340 NoHet case sets ϕ_{ClNO_2} to zero (i.e. $[\text{Cl}^-] = 0$ in Eq. 3 and 4) but keeps others the same as the Base case
341 so as to evaluate the importance of the of heterogeneous N_2O_5 + ClNO_2 chemistry (i.e., the model
342 sensitivities to a smaller gamma N_2O_5 and zero ClNO_2 production) through the comparison with the Base
343 case. Similarly, combined with three more sensitivity cases (NoChem, NoEmHet and NoAll, see details
344 in Table 2), the study provides an overall evaluation of the importance of tropospheric chlorine chemistry
345 as well as its sensitivities to chlorine emissions and the parameterizations for the heterogeneous N_2O_5 +
346 Cl chemistry N_2O_5 - ClNO_2 chemistry in the model.

347 2.2 Observations

348 Multiple observed data sets were applied in this study to evaluate the performance of GEOS-Chem
349 simulation, including the concentrations of chemical composition species of $\text{PM}_{2.5}$ from three
350 representative sites, located in south (Guangzhou, 23.14° N, 113.36° E), east (Dongying, 37.82° N, 119.05°
351 E) and north (Gucheng, 37.36° N, 115.96° E) China, respectively (Fig. S2). Concentrations of SO_4^{2-} , NO_3^- ,
352 NH_4^+ , Cl^- and organic matter (OM) in $\text{PM}_{2.5}$ were measured by High Resolution Time-of-Flight Aerosol
353 Mass Spectrometer (HR-ToF-AMS; Aerodyne Research Inc., USA, Decarlo et al. (2006)) from October
354 2 to November 18, 2018 (with a time resolution of 1 minute) at Guangzhou site (Chen et al., 2021b), and
355 from March 18 to April 21, 2018 (with a 1-minute time resolution) at Dongying site. Concentrations of
356 these species were measured by an Aerodyne Quadruple Aerosol Chemical Speciation Monitor (ACSM;
357 Aerodyne Research Inc., USA, Ng et al. (2011)) from November 11 to December 18 in 2018, with a time
358 resolution of 2 minutes at Gucheng site (Li et al., 2021).

359 Concentrations of N_2O_5 and ClNO_2 (with a time resolution of 1 minute) were also measured at
360 Guangzhou site by a Chemical Ionization Mass Spectrometer (CIMS, THS Instruments Inc., Atlanta,
361 (Kercher et al., 2009)) from September 25 to November 12 in 2018 (Ye et al., 2021). To have a thorough
362 evaluation of the representativeness of different parameterizations for $\gamma_{\text{N}_2\text{O}_5}$ and ϕ_{ClNO_2} , observations of
363 ClNO_2 and N_2O_5 at six more sites across China from previous studies (see Table S1-S2 and Fig. S2) are

带格式的: 字体: 倾斜

带格式的: 字体: 10 磅, 非加粗, 字体颜色: 红色

带格式的: 字体: 非倾斜

364 also used in this study. It should be noted that model results sampled at those sites for comparison were
365 simulated in the same months but different years while ignoring the uncertainties associated with the
366 interannual variability.

367 In addition, we also use observed hourly data of O₃ and PM_{2.5} published by the China National
368 Environmental Monitoring Center (CNEMC, <http://www.cnemc.cn/sss/>, last access on June 20, 2021)
369 to evaluate the model's overall performance in China. The network was launched in 2013 as part of the
370 Clean Air Action Plan, and includes ~1500 stations located in 370 cities by 2018 (Fig. S2).

371 3 Results and discussion

372 3.1 Improved model performance with updated chlorine emissions and [parameterizations for the](#) 373 [heterogeneous N₂O₅ + Cl chemistry](#) ~~N₂O₅ + ClNO₂ chemistry~~

374 Figure 2 shows time series of observed and simulated Cl⁻ concentrations at the Guangzhou, Dongying,
375 and Gucheng sites. The observations show the lowest Cl⁻ concentrations at the Guangzhou site ($0.55 \pm$
376 $0.52 \mu\text{g m}^{-3}$), although the site is the closest to the ocean among all three sites, while the highest
377 concentrations ($4.7 \pm 3.3 \mu\text{g m}^{-3}$) are observed at the Gucheng site, away from the sea. Moderate
378 concentrations of Cl⁻ is observed at the Dongying site, around $1.1 \pm 0.82 \mu\text{g m}^{-3}$. The relatively higher
379 concentrations observed inland again suggest the dominance of non-sea salt Cl⁻ in China, as mentioned
380 before in the Introduction.

381 The comparison between observations and simulated results from the NoEm case shows a serious
382 underestimate of Cl⁻ concentrations, with normalized mean bias (NMB) ranging from -96% to -79%,
383 suggesting the missing of significant chlorine sources in addition to sea salt chlorine. In contrast, the
384 Base case with updated chlorine emissions exhibits much higher Cl⁻ concentrations and can successfully
385 reproduce observations, with average [concentrations \(NMB\)](#) of 0.77 ± 0.54 ~~(-39%)~~, 0.71 ± 0.52 ~~(-36%)~~,
386 and $4.5 \pm 2.4 \mu\text{g m}^{-3}$ ~~(NMB = 39%, -36% and -4.7%)~~ ~~(-4.7%)~~ at the Guangzhou, Dongying, and Gucheng
387 sites, respectively. The increase in Cl⁻ concentrations in the Base case compared with the NoEm case is
388 the most significant at the Gucheng site, by a factor of 24 (from 0.19 to $4.5 \mu\text{g m}^{-3}$ on average). ~~The NMB~~

带格式的：下标

带格式的：下标

389 ~~in the Base case therefore has decreased to -36%—39%.~~The slight underestimates at the Dongying site
390 in the Base case could be to some extent explained by the bias in GFED4, which underestimates
391 emissions from agricultural fires due to their small size and short duration as suggested by the study of
392 Zhang et al. (2020). In spite of that, the model with the Base case well reproduces the overall distribution
393 of the observed particulate chloride concentrations in China. The correlation coefficients (r) between
394 observed and model results at the three sites also increase from -0.05 – 0.61 in the NoEm case to 0.40 –
395 0.71 in the Base case. The significant improvement in the model performance again suggests sources
396 other than SSA play a key role in Cl⁻ concentrations in China.

397 The comparison between observed and simulated N₂O₅ (Fig. 3a) shows that NMB for the NoEm case are
398 -58%, 150%, 108% and 25% at the Guangzhou, Wangdu, Taizhou and Mount Tai sites, respectively. In
399 contrast, the corresponding NMB for the Base case are much smaller, -57%, 48%, 91% and 18%,
400 respectively. ~~The improvement in the Base case is apparent at most sites, implying that additional~~
401 ~~chlorine emissions could effectively increase the uptake coefficient of N₂O₅ in: Yu parameterization. As~~
402 ~~shown in Figure S3, although the values of $\gamma_{N_2O_5}$ between the Base and NoEm cases are similar over the~~
403 ~~ocean, the Base case has rfrom the Base cases showed the highest value (0.016 averaged in China and~~
404 ~~up to 0.053 over the ocean on annual mean basis) in all simulation cases, while $\gamma_{N_2O_5}$ relatively higher~~
405 ~~$\gamma_{N_2O_5}$ over China compared with the from the NoEm case is little smaller (0.016 vs. 0.014 averaged in~~
406 ~~China and up to 0.053 over the ocean on annual mean basis) due to the smaller [Cl⁻] in Eq. 5. The~~
407 ~~improvement in the Base case is apparent at most sites, implying that additional chlorine emissions could~~
408 ~~effectively increase the uptake coefficient of N₂O₅. The improvement in the Base case is apparent at most~~
409 ~~sites, implying that additional chlorine emissions combined with the updated N₂O₅—ClNO₂ chemistry~~
410 ~~with Yu parameterization could effectively increase the uptake coefficient of N₂O₅. Little improvement~~
411 is found at the Guangzhou site (-58% in the NoEm case vs. -57% in the Base case). Previous studies also
412 found an underestimation of N₂O₅ in the Pearl River Delta (~~PRD~~), which could be partly explained by
413 the underestimation of the sources (e.g NO₂) and/or the overestimation of the sink of N₂O₅ there (Dai et
414 al., 2020; Li et al., 2016).

415 The N₂O₅ results from the McDuffie case, which uses ~~the~~ McDuffie parameterization (a default setting
416 in GEOS-Chem, see Section 2.1.1 and 2.1.3) instead of Yu parameterization are also shown in Fig. 3a.

417 The NMB for the McDuffie case are -53%, 154%, 143% and 37% at the Guangzhou, Wangdu, Taizhou
418 and Mount Tai sites, respectively. ~~The comparison between the McDuffie and Base cases indicates~~
419 ~~comparison indicates~~ that Yu parameterization can reproduce observed N_2O_5 better in China in general,
420 while McDuffie parameterization tends to overestimate N_2O_5 concentrations. ~~The overestimate of N_2O_5~~
421 ~~in McDuffie parameterization which could be mainly attributed to~~ suggests the potential underestimate
422 in the corresponding $\gamma_{\text{N}_2\text{O}_5}$. As shown Figure S344, the value of $\gamma_{\text{N}_2\text{O}_5}$ from the McDuffie case is much
423 smaller than that from the Base case (0.0071 vs. 0.016 averaged over China).

424 The underestimate in $\gamma_{\text{N}_2\text{O}_5}$ from the McDuffie case could to large extent be explained by the suppressive
425 effect of organic coatings (γ_{coat}) as discussed above in Section 2.1.1. ~~Our model simulation shows the value~~
426 ~~of $\gamma_{\text{N}_2\text{O}_5}$ from the McDuffie case (0.0071 averaged in China and up to 0.037 over the ocean on annual~~
427 ~~mean basis) is significantly smaller than that from the Base case (Fig. S11), due to the overprediction of~~
428 ~~organic coating suppression level and lack of chloride enhancement in $\gamma_{\text{N}_2\text{O}_5}$ from McDuffie~~
429 ~~parameterization (as discussed in Section 2.1.1). the overprediction of organic coating suppression level~~
430 ~~in China. The suppression of organic coating in McDuffie parameterization (γ_{coat} , Eq. 3) is calculated as~~
431 ~~a function of organic aerosol O:C ratio and RH, which could comprehensively account for the~~
432 ~~suppression of organic aerosol on N_2O_5 uptake under various ambient conditions and aerosol phase (as~~
433 ~~discussed in Section 2.1.1). However, the magnitude of the organic suppression is highly dependent on~~
434 ~~many factors (e.g. organic composition, particle phase state, etc.) and thus remains poorly quantified~~
435 ~~(Griffiths et al., 2009; Gross et al., 2009; Thornton et al., 2003). Although many studies have shown that~~
436 ~~organic aerosol can suppress the N_2O_5 uptake (Anttila et al., 2006; Riemer et al., 2009ref), the level of~~
437 ~~organic suppression may be overpredicted while currently in currently implemented parameterization~~
438 ~~implemented parameterization may overpredict the level of suppression due attributed to the poorly~~
439 ~~quantified and/or unknown to these factors remain poorly quantified (e.g. Morgan et al. (2015)). On the~~
440 ~~other hand~~ For example, some studies found that ignoring the difference ~~the model does not differentiate~~
441 ~~precisely between water-soluble and water-insoluble organics fractions, which may also lead to an upper~~
442 ~~limit for estimating the suppressive effect of an organic coatings and consequently an underestimate in~~
443 ~~the solubility and diffusivity of N_2O_5 in organic matter (e.g. Chang et al., (2016); Yu et al., 2020).~~
444 Although the γ_{coat} in McDuffie parameterization is calculated as a function of organic aerosol O:C ratio
445 and RH (see Eq. 2), which could increase with higher RH and higher O:C ratio, it may still overpredict

带格式的：下标

带格式的：下标

带格式的：下标

带格式的：下标

带格式的：字体：非倾斜

带格式的：字体：非倾斜

带格式的：字体：非倾斜

446 the suppressive role of organic coatings in China. On the other hand, the study by Yu et al. (2020) found
447 that excluding the organic coating best reproduced uptake coefficients observed in China. In addition,
448 the bias underestimate in $\gamma_{\text{N}_2\text{O}_5}$ in McDuffie parameterization in China also could also be to some extent
449 explained by the fact that the parameterization the lack of the does not consider chloride enhancement
450 (as also discussed in Section 2.1.1). It is worth noting that the evaluation here is specific to China and the
451 differences between Yu and McDuffie parameterizations have not been evaluated elsewhere.

带格式的: 字体: 非倾斜

带格式的: 字体: 倾斜

带格式的: 字体: 非倾斜

452 Both of these reasons lead to an underprediction of $\gamma_{\text{N}_2\text{O}_5}$ in McDuffie parameterization in this study.
453 suppression from the organic coatings leading to a much lower $\gamma_{\text{N}_2\text{O}_5}$ (see Eq. 1 for McDuffie
454 parameterization). Similarly, Morgan et al. (2015) found significant underestimates in $\gamma_{\text{N}_2\text{O}_5}$ when the
455 effect of organic coatings is considered. The effect of organic coatings strongly depends on organic
456 composition, particle phase state, and the environmental factors (e.g. RH and temperature), and thus
457 remains poorly quantified (McDuffie et al., 2018b; Morgan et al., 2015). As suggested by the study of Yu
458 et al. (2020), the bias in $\gamma_{\text{N}_2\text{O}_5}$ in McDuffie parameterization could be to some extent explained by the
459 fact that the parameterization does not differentiate between water-soluble and water-insoluble organic
460 fractions and simplifies the morphology and phase state, resulting in an underestimation of the solubility
461 and the diffusivity of N_2O_5 in organic matter.

462 For the comparison of ClNO_2 (Fig. 3b), we use the mean nighttime (excluding the data at local time of
463 10:00 – 16:00) maximum mixing ratio, as suggested by Wang et al. (2019b and 2020b). Observed ClNO_2
464 is high in Guangzhou (1121 pptv) and Wangdu (~ 990 pptv), followed by Changping (~ 500 pptv) and
465 Beijing (~ 430 pptv). The lowest concentrations are obtained at Mount Tai and Mount TaiMoShan (~ 150
466 and 120 pptv, respectively) due to relatively clean condition at high altitude. The comparison between
467 observed and simulated ClNO_2 at different sites also suggests a better model performance for the Base
468 case with NMB in the range of -28% – 22%, compared with the NMB of -77% – -31% and -59% – -36%
469 for the NoEm and McDuffie cases, respectively. The difference in ClNO_2 concentrations is mainly
470 associated with distinct ϕ_{ClNO_2} values among different cases. As shown in Figure: S412, the value of
471 ϕ_{ClNO_2} is significantly higher in the Base case (0.36 averaged over China) than in the NoEm (0.14) and
472 McDuffie (0.11) cases. Figure S12 presents the spatial distribution of annual mean ϕ_{ClNO_2} in the model
473 surface layer from different simulation cases. Results show that the value of ϕ_{ClNO_2} are significantly

474 higher than the NoEm and McDuffie cases, with annual mean value of 0.36, 0.14 and 0.11 averaged in
475 China, respectively. The large difference between the NoEm and Base cases in the inland China again
476 emphasizes the important role of non-sea salt chlorine in the formation of ClNO₂. The overall
477 underestimates in McDuffie parameterization on the other hand may suggest that the scaling factor of
478 0.25 and the coefficient of k_2/k_1 (1/450) applied to ϕ_{ClNO_2} in Eq. 2-4 is too much is not appropriate for the
479 atmospheric condition in China. More field measurements and model evaluations are required to come
480 up with a more precise parameterization better representing ϕ_{ClNO_2} in China.

带格式的: 字体: 倾斜

带格式的: 下标

带格式的: 字体: 倾斜

带格式的: 下标

带格式的: 字体: 倾斜

481 A scaling factor of 0.5 instead of 0.25 may fit better with observations used in the study. More field
482 measurements and model evaluations are required to come up with a more precise scaling factor better
483 representing ϕ_{ClNO_2} in China. Overall, with updated chlorine emissions and Yu parameterization for $\gamma_{\text{N}_2\text{O}_5}$
484 and ϕ_{ClNO_2} , the Base case agrees better with both the magnitude and the spatial variation of observed
485 N₂O₅ and ClNO₂ in China.

486 The differences in $\gamma_{\text{N}_2\text{O}_5}$ and ϕ_{ClNO_2} could also lead to variations of affect the ratios of ClNO₂ to HNO₃
487 production through the NO_x circulation. As shown in Figure S5, shows the ratio value of ClNO₂ to
488 HNO₃ from the Base case is the highest from the Base case (9.8% averaged in China and up to 47% in
489 the Sichuan Basin on annual mean basis), while followed by that from the McDuffie (4.7% averaged
490 in China and up to 18% in the Sichuan Basin) and NoEm (3.1% averaged in China and up to 12% in
491 coastal regions) cases and McDuffie (4.7% averaged in China and up to 18% in the Sichuan Basin on
492 annual mean basis) cases are significantly smaller due to both lower values of $\gamma_{\text{N}_2\text{O}_5}$ and ϕ_{ClNO_2} .

带格式的: 下标

493 To further elucidate how the model behaves in reproducing the spatial distribution of ozone and PM_{2.5}
494 through the incorporation of the additional chlorine emissions and updated Yu parameterization for s of
495 the heterogeneous N₂O₅ + ClNO₂ chemistry with Yu parameterization, simulated MDA8 O₃ and PM_{2.5}
496 from different cases were compared with observations across China. Figure 4 shows observed-simulated
497 annual mean MDA8 O₃ and PM_{2.5} in 2018 in China from the Base case compared with the observations
498 from CNEMC (China National Environmental Monitoring Center, as introduced at in Section 2.2)
499 compared with the model results from the Base case. The observed annual mean MDA8 O₃ and PM_{2.5}
500 are 49 ppbv and 39 $\mu\text{g m}^{-3}$ respectively in 2018 in China. Model results from the Base case could
501 generally reproduce observed spatial and seasonal variations of annual mean MDA8 O₃ and PM_{2.5}

502 concentrations, with NMB of -26% and 3.6% and r of 0.83 and 0.81 respectively (~~correlation coefficients~~
503 ~~maps of MDA8 O₃ and PM_{2.5} are shown at Fig. S36~~).

504 Table 3 also summarized the model performance on both annual and seasonal scales regarding the
505 simulation of O₃ and PM_{2.5} from different cases. For the comparison with observed MDA8 O₃, although
506 different simulation cases show a similar range of r , the Base case tends to have a slightly smaller bias
507 in general, with NMB of -26% on annual average (-49% – -5.5% on seasonal mean) vs. -28% (-54% – -
508 5.9%) in the NoEm and -27% (-53% – -5.2%) in the McDuffie case. For the comparison with observed
509 PM_{2.5}, the NMB bias from the Base case is 3.6% on annual average (-6.3% – 28% on seasonal mean).
510 Compared with the NoEm case, there is some improvement in summer (5.0% vs. 3.9%) and winter (-
511 7.9% vs. -4.3%) but slightly larger bias in autumn (26% vs. 28%). The McDuffie case on the other hand
512 produces slightly higher PM_{2.5} concentrations, with NMB of 5.6%. Regarding the ~~simulation of~~
513 ~~particulate-chemical composition species of PM_{2.5}~~ (Table S2S3), although the model performance varies
514 with sites and species, the Base case demonstrates better agreement with observations compared with the
515 NoEm and McDuffie cases in general.

516 On the whole, the model performance is better with the additional anthropogenic and biomass burning
517 chlorine emissions combined with ~~Yu updated parameterization for the of -heterogeneous N₂O₅ + Cl~~
518 ~~chemistry N₂O₅ – ClNO₂ chemistry represented by Yu parameterization~~. Therefore, the following
519 investigation of the impacts of chlorine chemistry on air quality in China as well as their sensitivities to
520 chlorine emissions and parameterizations for ~~the heterogeneous N₂O₅ + Cl chemistry N₂O₅ – ClNO₂~~
521 ~~chemistry~~ is mainly based on the Base case.

522 3.2 Impacts of tropospheric chlorine chemistry on air quality and the role of the heterogeneous 523 N₂O₅ + ClNO₂ chemistry

524 To comprehensively quantify the importance of chlorine chemistry, we conducted a sensitivity case in
525 which all related tropospheric chlorine chemistry was turned off (NoChem, also listed in Table 2). The
526 differences between the Base and NoChem cases (Fig. 5 and Fig. S3S74) could thus represent the impact
527 of the chlorine chemistry. The comparison shows that chlorine chemistry could increase annual mean
528 nighttime max ClNO₂ surface concentrations by 243 pptv averaged in China (up to 1548 pptv in the

带格式的: 字体: 10 磅, 非加粗

带格式的: 下标

带格式的: 下标

529 [SCBSichuan Basin](#)). The increase in annual mean Cl atoms is 1.7×10^3 molec cm^{-3} averaged in
 530 [ChianChina](#) (up to 7×10^3 molec cm^{-3} in coastal regions); ~~The reaction increased of Cl atoms and could~~
 531 ~~react with VOCs (especially alkanes) producing produces additional more organic peroxyperoxy radicals,~~
 532 ~~including organic peroxy radicals (RO_2) and , which are then rapidly reeyeled to hydroperoxyl radicals~~
 533 ~~(HO_2). -As shown in Figure- S74 (a). Results show that the chlorine chemistry could increase annual~~
 534 ~~mean HO_2 concentrations by 1.6×10^6 molec cm^{-3} averaged in China (up to 8.6×10^6 molec cm^{-3} in~~
 535 ~~the coastal regions). In the presence of NO , the peroxy radicals recycle OH while oxidize NO to NO_2 .~~
 536 ~~The subsequent photolysis of NO_2 could further lead to more O_3 production and consequently also more~~
 537 ~~OH (Osthoff et al., 2008; Riedel et al., 2014; Simpson et al., 2015ref). On the other hand, the recycling~~
 538 ~~of NO_x back into the atmosphere associated with the photolysis of ClNO_2 could also lead to more O_3~~
 539 ~~production. The increased HO_2 subsequently oxidized NO to NO_2 , whiThe results here show a significant~~
 540 ~~eh-increase in surface annual mean OH (Fig. S74 (b)) and MDA8 O_3 significantly (Fig. 5c) by $3.8 \times$~~
 541 ~~10^4 molec cm^{-3} and 1.1 ppbv respectively averaged in China (up to 1.2×10^5 molec cm^{-3} andwith annual~~
 542 ~~mean concentrations of 1.1 ppbv in China and by as much as 4.5 ppbv respectively in the Sichuan Basin)~~
 543 ~~(Fig. 5c). Ultimately, the surface OH concentration was increased significantly through NO oxidation~~
 544 ~~and O_3 photolysis, with an annual average of 3.8×10^4 molec cm^{-3} in Chian while by up to 1.2×10^5~~
 545 ~~molec cm^{-3} in the Sichuan Basin, which further lead to an increase in surface annual mean MDA8 O_3 and~~
 546 ~~OH by 1.1 ppbv and 3.8×10^4 molec cm^{-3} averaged in China (up to 4.5 ppbv and 1.2×10^5 molec cm^{-3} in~~
 547 ~~the SCB) respectively through VOCs oxidation. In contrast, annual mean $\text{PM}_{2.5}$ surface concentrations~~
 548 are decreased by $0.91 \mu\text{g m}^{-3}$ averaged in China (up to $7.9 \mu\text{g m}^{-3}$ in the [SCBSichuan Basin](#)), mainly due
 549 to the decrease of NO_3^- and NH_4^+ (up to $6.4 \mu\text{g m}^{-3}$ and $1.9 \mu\text{g m}^{-3}$ respectively), although SO_4^{2-}
 550 concentrations are increased slightly by up to $1.2 \mu\text{g m}^{-3}$ in the [SCBSichuan Basin](#) (Fig. [S3S74](#)).

551 ~~The composition and partitioning of total reactive nitrogen (NO_x) affect the spatial range that nitrogenous~~
 552 ~~species can reach after emission, and they are therefore of great importance in atmospheric chemistry~~
 553 ~~(Bertram et al., 2012). Chlorin chemistry affects the fate and composition of NO_x through the recycling~~
 554 ~~of NO_x and nitrate production (e.g. (Li et al. (2016); Wang et al. (2020a))). Our results show that chlorine~~
 555 ~~chemistry in China could increase the ratio of NO_x ($= \text{NO} + \text{NO}_2 + \text{ClNO}_2$) to NO_x (2.1% averaged in~~
 556 ~~China and up to 5.7% in the Sichuan Basin, Northeast Plain and North China Plain on annual mean basis)~~
 557 ~~due to more NO_2 and ClNO_2 production, but decrease ratio of NO_x to NO_x (1.3% averaged in China and~~

带格式的：下标

带格式的：非上标/下标

带格式的：下标

带格式的：字体：10 磅

带格式的：下标

带格式的：下标

带格式的：下标

域代码已更改

带格式的：下标

带格式的：下标

带格式的：下标

带格式的：下标

带格式的：下标

带格式的：下标

带格式的：下标

带格式的：上标

带格式的：下标

558 ~~up to 5.2% in the Sichuan Basin on annual mean basis) (Fig. S5).~~

559 Previous studies suggested that tropospheric chlorine drives a global decrease of O₃ by catalytic

560 production of bromine and iodine radicals from hypohalous acids (HOX, where X = Br and I) (Schmidt

561 et al., 2016; Wang et al., 2019). On the contrary, Both global and regional studies suggested ~~that that the~~

562 heterogeneous N₂O₅ + ClNO₂ chemistry can enhance O₃ production through the production of Cl

563 atoms and the recycling of NO_x (Li et al., 2016; Sarwar et al., 2014; Wang et al., 2019). Therefore, we

564 further investigate the role that the heterogeneous N₂O₅ + ClNO₂ chemistry plays in tropospheric

565 chlorine chemistry through the comparison between the Base and NoHet (Fig. 6 and Fig. S4S86) cases.

566 Keep it in mind that the comparison is mainly assessing the impact of ClNO₂ production, namely the

567 uptake of N₂O₅ on chloride aerosol, not the general role of N₂O₅ heterogeneous chemistry. The

568 comparison illustrates that the heterogeneous N₂O₅ + ClNO₂ chemistry could result in a

569 significant production of ClNO₂, reaching 600 – 1400 pptv for annual mean nighttime max surface

570 concentrations in the North China PlainNCP, and up to 1546 pptv in the SCBSichuan Basin. The change

571 in the surface concentrations of Cl atoms (an annual mean increase of 1 – 4 × 10³ molec cm⁻³ in central

572 and eastern China) is mainly due to the photolysis of ClNO₂ and accounts for 74% of total change in

573 annual mean Cl atoms due to all tropospheric chlorine chemistry in China, which are consistent with the

574 results from the previous study by Liu et al. (2017).

575 In addition to the production of Cl atoms, the ClNO₂ formation also affects the partitioning of NO_y from

576 HNO₃ into more reactive forms (e.g., NO_x and ClNO₂) through the recycling of NO_x, and thereforeThe

577 composition and partitioning of total reactive nitrogen (NO_y) affect the spatial range that nitrogenous

578 species can reach after emission, and they are therefore of great importance in atmospheric chemistry

579 (Bertram et al., 2013; Li et al., 2016; Wang et al., 2020a). Chlorin chemistry affects the fate and

580 composition of NO_y through the recycling of NO_x and nitrate production (e.g., (Li et al. (2016); Wang et

581 al. (2020a)).). To analyze the impact of the heterogeneous N₂O₅ + Cl chemistry on NO_y partitioning,

582 Figure S95 shows the change in the ratios of NO_x to NO_y and NO₃ to NO_y as the difference between the

583 Base and NoHet cases. Since ClNO₂ could be treated as a reservoir for reactive nitrogen at night, we

584 include ClNO₂ as part of NO_x in the calculation (NO_x = NO + NO₂ + ClNO₂ and NO_y = NO + NO₂ +

585 ClNO₂ + HNO₃ + 2 × N₂O₅ + NO₃ + HONO + HNO₄ + NO₃⁻ + various organic nitrates). OurThe results

带格式的：字体：非倾斜
带格式的：非上标/下标

带格式的：段落间距段前：12 磅

带格式的：字体：10 磅，非倾斜

带格式的：字体：10 磅，非倾斜，下标

带格式的：字体：10 磅，非倾斜

带格式的：字体：10 磅

带格式的：字体：10 磅，下标

带格式的：字体：10 磅

带格式的：字体：10 磅，下标

带格式的：字体：10 磅

带格式的：字体：10 磅，下标

带格式的：字体：10 磅

带格式的：字体：10 磅

域代码已更改

带格式的：字体：10 磅

域代码已更改

带格式的：字体：10 磅

带格式的：字体：10 磅

带格式的：下标

带格式的：下标

带格式的：下标

带格式的：下标

带格式的：非上标/下标

带格式的：下标

带格式的：下标

带格式的：下标

带格式的：下标

带格式的：下标

带格式的：下标

带格式的：上标

586 ~~show that due to the ClNO₂ production, chlorine chemistry in China could increase the ratios of NO_x (=~~
587 ~~NO + NO₂ + ClNO₂) to NO_y increase by 2.18% averaged in China and up to 5.74% in the Sichuan~~
588 ~~Basin, Northeast Plain and North China Plain on annual mean basis. Meanwhile,) due to more NO₂ and~~
589 ~~ClNO₂ production, but decrease the ratios of NO₃⁻ to NO_y decrease by 1.31% averaged in China and up~~
590 ~~to 5.21% in the Sichuan Basin on annual mean basis) (Fig. S5).~~

591

592 Consequently, the annual mean MDA8 O₃ surface concentrations are increased by 1.5 – 3 ppbv in central
593 and eastern China and by up to 3.8 ppbv in the SCBSichuan Basin, accounting for 83% of total change
594 in annual mean MDA8 O₃ due to all tropospheric chlorine chemistry in China. It is interesting to note
595 that while MDA8 O₃ surface concentrations show maxima in summer and minima in winter in general,
596 the influence of the heterogeneous N₂O₅ + ClN₂O₅ – ClNO₂ chemistry on O₃ concentrations exhibits a
597 different seasonality. The increase in seasonal mean MDA8 O₃ concentrations is the largest in winter (by
598 up to 6.5 ppbv in the SCBSichuan Basin); but is less than 1.5 ppbv in summer. This is because of more
599 accumulation of N₂O₅ and ClNO₂ in dark conditions in long winter nights (Sarwar et al., 2014).

600 There also exhibits an obvious decrease in the annual mean surface concentrations of PM_{2.5} attributed to
601 the heterogeneous N₂O₅ + ClN₂O₅ – ClNO₂ chemistry, ranging from 1.5 to 4.5 μg m⁻³ in central and
602 eastern China (accounting for 90% of total change in annual mean PM_{2.5} due to all tropospheric chlorine
603 chemistry in China). The decrease is more significant in autumn and winter in China, with a range of 3.5
604 – 5.5 μg m⁻³ in central and eastern China; and being up to 11 μg m⁻³ in the SCBSichuan Basin. In contrast,
605 the decrease in PM_{2.5} is less than 2 μg m⁻³ in summer in China. The change in PM_{2.5} is mainly due to the
606 decrease in NO₃⁻ (up to 6.2 μg m⁻³ in the SCBSichuan Basin on annual average). In addition, NH₄⁺ is
607 also decreased by up to 1.8 μg m⁻³ in the SCBSichuan Basin on annual average, following the pattern of
608 ΔNO₃⁻. This is because NH₃ is in excess in most regions in China (Xu et al., 2019) and the formation of
609 ClNO₂ via R2 could hinder the formation of HNO₃ and shift the partitioning between NH₃ and NH₄⁺
610 towards NH₃. Unlike the change in NO₃⁻ and NH₄⁺, the heterogeneous N₂O₅ + ClN₂O₅ – ClNO₂
611 chemistry increases surface SO₄²⁻ concentration slightly, which could be explained by the enhancements
612 of atmospheric oxidation associated with the increase in Cl atoms, OH and O₃, facilitating the formation
613 of secondary aerosols (Sarwar et al., 2014).

614 On the other hand, ~~the comparison between the NoHet and NoChem cases indicate~~ the effect of
615 tropospheric chlorine chemistry without the [heterogeneous \$N_2O_5 + ClN_2O_5 - ClNO_2\$](#) chemistry is much
616 smaller (Fig. [S5S107, the comparison between the NoHet and NoChem cases](#)), leading to an increase of
617 up to 0.7 ppbv in inland China and a decrease of 0.3 – 0.5 ppbv in coastal regions for annual mean MDA8
618 O_3 concentrations. The increase is probably associated with Cl atoms from photolysis of gas-phase
619 chlorine, especially non-sea salt Cl_2 in inland China, while the decrease at coastal regions is mainly due
620 to catalytic production of bromine and iodine radicals originated from sea-salt aerosols. The comparison
621 demonstrates the dominance of [the heterogeneous \$N_2O_5 + ClN_2O_5 - ClNO_2\$](#) chemistry in total
622 tropospheric chlorine chemistry in China.

623 3.3 The effect of [heterogeneous \$N_2O_5 + ClN_2O_5 - ClNO_2\$](#) chemistry in response to chlorine emissions

624 Since both $\gamma_{N_2O_5}$ and ϕ_{ClNO_2} in the Yu parameterization are highly dependent on $[Cl]$, the effect of [the](#)
625 [heterogeneous \$N_2O_5 + ClN_2O_5 - ClNO_2\$](#) chemistry on air quality is thus sensitive to chlorine emissions.
626 Figure 7 shows the effects of [the](#) additional chlorine emissions from anthropogenic and biomass burning
627 sources on annual mean surface concentrations of different species (Cl^- , Cl atom, OH, MDA8 O_3 , $PM_{2.5}$
628 and NO_3^-) in China, calculated as the differences between the Base and the NoEm case. With the
629 implementation of the additional chlorine emissions, the particulate Cl^- concentration increased
630 significantly in inland China, with the largest increase in the [SCBSichuan Basin](#) ($4.5 \mu g m^{-3}$) and little
631 change in west China. The increase is in the range of $1.5 - 3.5 \mu g m^{-3}$ in the [North China PlainNCP](#) and
632 $< 0.5 \mu g m^{-3}$ in South China. The spatial distribution of ΔCl atoms is also consistent with that of the
633 additional chlorine emissions and ΔCl , showing the largest increment in the [SCBSichuan Basin](#) (about
634 $4.5 - 5 \times 10^3 molec cm^{-3}$). There is also a moderate increase in Cl atoms in the [Northeast PlainNP](#) and
635 [North China PlainNCP](#), with a range of $1.5 - 4 \times 10^3 molec cm^{-3}$. Only a minor increase of Cl atoms is
636 found in South China ($< 1 \times 10^3 molec cm^{-3}$).

637 ~~As discussed earlier in Section 3.2, increased Cl atoms could lead to more HO_2 and OH via VOCs~~
638 ~~oxidation. Combined with increased NO_3^- associated with the release of NO_2 upon the photolysis of~~
639 ~~$ClNO_2$, further increases in both O_3 and OH could also be expected. The reactions of VOCs with Cl~~
640 ~~atoms lead to a further increase in HO_2 , which increase O_3 production and ultimately lead to an increase~~
641 ~~in OH is around (an annual mean increase of $2 - 9 \times 10^4 molec cm^{-3}$ in central and eastern China on~~

带格式的：下标

带格式的：下标

带格式的：下标

带格式的：下标

带格式的：下标

带格式的：上标

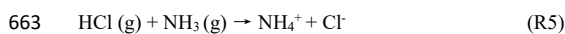
带格式的：上标

带格式的：下标

642 ~~annual mean basis) through NO oxidation and O₂ photolysis (as discussed in section 3.2)~~The reactions
643 ~~of VOCs with Cl atoms lead to a further increase in OH (an annual mean increase of 2–9 × 10⁴ molec~~
644 ~~em⁻³ in central and eastern China) and O₃. The increase in O₃ could also be due to the recycling of NO_x~~
645 ~~back to the atmosphere associated with the photolysis of ClNO₂ (R4).~~ The increase in MDA8 O₃ surface
646 concentrations ranges from 0.5 to 3 ppbv in central and eastern China, and reaches up to 3.5 ppbv in the
647 [SCBSichuan Basin](#) on annual average. The impacts of chlorine sources on O₃ formation also vary with
648 seasons. Although O₃ pollution is generally severe in summer, the change in MDA8 O₃ due to [the](#)
649 [additional](#) chlorine sources is relatively minor, with maxima of 0.7 ppbv in the [SCBSichuan Basin](#) and <
650 0.5 ppbv in most other regions averaged in summer. In contrast, the increase is most obvious in winter,
651 with maxima of 5.2 ppbv in the [SCBSichuan Basin](#) on seasonal average.

652 The effects of the additional chlorine emissions on surface PM_{2.5} concentrations ~~is~~are complicated. The
653 [North China Plain NCP](#) shows the largest increase (3–4.5 μg m⁻³ on annual average), mainly due to the
654 increase in Cl⁻, which could also promote [the heterogeneous N₂O₅ + ClN₂O₅ → ClNO₂](#) chemistry and lead
655 to more NO₃⁻ production (Chen et al., 2021a). In contrast, the [SCBSichuan Basin](#) exhibits both an
656 increase (by up to 4.2 μg m⁻³) and a decrease (by up to 3.7 μg m⁻³). The decrease of PM_{2.5} in the
657 [SCBSichuan Basin](#) is mainly due to the large decrease of NO₃⁻ there. In the [SCBSichuan Basin](#), nitrate
658 formation is dominated by the heterogeneous hydrolysis of N₂O₅ (Tian et al., 2019) while the additional
659 Cl⁻ could hinder the path of N₂O₅ hydrolysis due to [the](#) competition with the path of ClNO₂ formation.
660 Consequently, the additional chlorine emissions result in a decrease of NO₃⁻ up to 5.6 μg m⁻³ in [the](#)
661 [SCBSichuan Basin](#) on annual average.

662 In addition, NH₄⁺ concentrations could also be affected through the reaction of R5:



664 In the [Northeast Plain NP](#) and [North China Plain NCP](#) where anthropogenic and biomass burning
665 emissions of HCl are high, the annual mean NH₄⁺ surface concentrations are increased by 0.5–1.5 μg
666 m⁻³ (Fig. [S6S11 \(a\)8](#)). NH₄⁺ concentrations are also affected by the gas-particle partitioning equilibrium,
667 and decrease as the pH value gets higher (or increase with H⁺ concentrations). Therefore, the competition
668 between the [heterogeneous N₂O₅ + ClN₂O₅ → ClNO₂](#) chemistry and N₂O₅ hydrolysis could also affect the
669 formation of NH₄⁺. In other words, increased Cl⁻ concentrations could result in less H⁺ and thus less

670 NH_4^+ . Consequently, there also exists some decrease in NH_4^+ concentrations in the [SCBSichuan Basin](#)
671 associated with the large decrease in NO_3^- concentrations. In contrast, little change is found for surface
672 SO_4^{2-} concentrations, less than $0.5 \mu\text{g m}^{-3}$ in most regions of China (Fig. [S6S11 \(b\)](#)).

673 It is worth mentioning that the effects of the additional chlorine emissions work mainly through the
674 [heterogeneous \$\text{N}_2\text{O}_5 + \text{ClN}_2\text{O}_5 \rightarrow \text{ClNO}_2\$](#) chemistry. Without this heterogeneous chemistry, the increase
675 of chlorine emissions shows only a minor change in Cl atoms ($< 10^3 \text{ molec cm}^{-3}$ in China, estimated as
676 the difference between the NoHet and NoEmHet cases in Fig. [S7S129](#)). The impact of chlorine emissions
677 on O_3 concentrations also weakens when the [heterogeneous \$\text{N}_2\text{O}_5 + \text{ClN}_2\text{O}_5 \rightarrow \text{ClNO}_2\$](#) chemistry is turned
678 off, with an increase of $0.5 - 1 \text{ ppbv}$ in MDA8 O_3 on annual average (vs. $0.5 - 3 \text{ ppbv}$ mentioned above).

679 On the other hand, the impacts of [heterogeneous \$\text{N}_2\text{O}_5 + \text{ClN}_2\text{O}_5 \rightarrow \text{ClNO}_2\$](#) chemistry on air quality in
680 inland China would be seriously underestimated if the additional anthropogenic and biomass burning
681 chlorine sources are ignored. If only sea salt chlorine emission is included in the simulation, the increase
682 of ClNO_2 surface concentrations resulted from [heterogeneous \$\text{N}_2\text{O}_5 + \text{ClN}_2\text{O}_5 \rightarrow \text{ClNO}_2\$](#) chemistry only
683 occurs in coastal regions due to the heterogeneous uptake of N_2O_5 on sea salt chloride aerosols (by up to
684 260 pptv on annual average, indicated by the difference between the NoEm and NoEmHet cases, Fig.
685 [S8S130](#)). Consequently, the increase in Cl atoms and MDA8 O_3 surface concentrations is found mainly
686 in coastal regions. For instance, annual mean MDA8 O_3 concentrations are increased by up to 2 ppbv in
687 coastal regions, but by less than 0.5 ppbv in inland China. In other words, the dominance of [the](#)
688 [heterogeneous \$\text{N}_2\text{O}_5 + \text{ClN}_2\text{O}_5 \rightarrow \text{ClNO}_2\$](#) chemistry in the impact of chlorine chemistry on air quality in
689 China is to large extent driven by the additional chlorine emissions.

690 **3.4 The effect of [heterogeneous \$\text{N}_2\text{O}_5 + \text{ClN}_2\text{O}_5 \rightarrow \text{ClNO}_2\$](#) chemistry in response to parameterizations** 691 **for $\gamma_{\text{N}_2\text{O}_5}$ and ϕ_{ClNO_2}**

692 ~~As shown in Figure S11 and S12, the value of $\gamma_{\text{N}_2\text{O}_5}$ presents the spatial distribution of annual mean $\gamma_{\text{N}_2\text{O}_5}$ and~~
693 ~~ϕ_{ClNO_2} in the model surface layer from different simulation cases, respectively. $\gamma_{\text{N}_2\text{O}_5}$ from the Base cases~~
694 ~~(Yu parameterization) showed the highest value (0.016 averaged in China and up to 0.053 over the ocean~~
695 ~~on annual mean basis) in all simulation cases, while $\gamma_{\text{N}_2\text{O}_5}$ from the NoHet and NoChem cases are smaller~~
696 ~~(0.014 averaged in China and up to 0.052 over the ocean on annual mean basis) than that from the Base~~

697 case (0.016 averaged in China and up to 0.053 over the ocean on annual mean basis), which suggests that
698 the heterogeneous uptake of N_2O_5 on chloride-containing aerosol surfaces in the Yu parameterization is
699 an important loss pathway of N_2O_5 , and should not be ignored. On the other hand,

700 It should be noted that the impact of the heterogeneous $N_2O_5 + ClN_2O_5 \rightarrow ClNO_2$ chemistry on air quality
701 not only depends on the amount of chlorine emissions, but is also sensitive to the parameterizations for
702 $\gamma_{N_2O_5}$ and ϕ_{ClNO_2} . Compared with the Base cases, $\gamma_{N_2O_5}$ and ϕ_{ClNO_2} from the NoEm cases are much smaller
703 (0.014 and 0.14 averaged in China on annual mean basis, respectively) due to smaller $[Cl^-]$ in Eq. 5. The
704 differences in $\gamma_{N_2O_5}$ and ϕ_{ClNO_2} between the Base and NoEm cases lead to variations of the ratio of $ClNO_2$
705 to HNO_2 production. Figure S13 shows the ratio of $ClNO_2$ to HNO_2 from the Base case is the highest
706 (9.8% averaged in China and up to 47% in the Sichuan Basin on annual mean basis), while that from the
707 NoEm cases is significantly smaller (3.1% averaged in China and up to 12% in coastal regions). As
708 discussed earlier (Fig. 3a), there exists a large difference in simulated N_2O_5 between the Base and NoEm
709 cases at the Wangdu site, implying the sensitivity of $\gamma_{N_2O_5}$ to chlorine emissions in the Yu
710 parameterization and thus the importance of non-sea salt chlorine emissions in China. This is consistent
711 with the dependence on chloride in Yu parameterization, which is included to better reproduce $\gamma_{N_2O_5}$
712 observations in China (Yu et al., 2020). The comparison between the Base and NoHet cases ($\gamma_{N_2O_5} =$
713 0.016 and 0.014, respectively not shown here) also suggests that the heterogeneous uptake of N_2O_5 on
714 chloride-containing aerosol surfaces in the Yu parameterization is an important loss pathway of N_2O_5 ,
715 and N_2O_5 and should not be ignored.

716 On the other hand, the value of $\gamma_{N_2O_5}$ from the McDuffie case is significantly smaller (0.0071 averaged
717 in China and up to 0.037 over the ocean on annual mean basis) than that from the Base case, due to the
718 overprediction of organic coating suppression level and lack of chloride enhancement in $\gamma_{N_2O_5}$ from
719 McDuffie parameterization (as discussed in Section 3.1) (Fig. S11). The value of ϕ_{ClNO_2} from the
720 McDuffie case is also smaller than that of the Base case (0.11 averaged in China and up to 0.25 on annual
721 mean basis) (Fig. S12) due to the scaling factor (i.e. 0.25) and smaller k_2/k_3 in Eq. 4. Both lower values
722 of $\gamma_{N_2O_5}$ and ϕ_{ClNO_2} lead to a smaller ratio of $ClNO_2$ to HNO_2 in the McDuffie cases (4.7% averaged in
723 China and up to 18% in the Sichuan Basin on annual mean basis) (Fig. S13).

724 In contrast to the Yu parameterization, N_2O_5 concentrations have little dependence on chlorine

带格式的: 非突出显示

带格式的: 非上标/下标

带格式的: 字体: (默认) Times New Roman, 10 磅

带格式的: 下标

带格式的: 下标

725 emissions in ~~the~~ McDuffie parameterization (Fig. 3a). This insensitivity to chlorine emissions could be
726 expected from Eq. 2 where ~~the that $\gamma_{\text{Cl}}^{\text{Cl}}^{\text{Cl}}$ in McDuffie parameterization does not include any dependence~~
727 ~~on aerosol chloride is not included so as to better reproduce wintertime reactive nitrogen observations in~~
728 ~~the eastern U.S.(Eq. 2), because they found it could fit their observations better (as discussed in Section~~
729 ~~2.1.1).~~ ~~from Eq. 1 where $\gamma_{\text{N}_2\text{O}_5}$ relies mainly on total concentrations of inorganic species, of which~~
730 ~~chlorine is only a minor component.~~ The ~~smaller-little~~ dependence of $\gamma_{\text{N}_2\text{O}_5}$ on concentrations of Cl⁻
731 together with the lower value of ϕ_{ClNO_2} make the results from the McDuffie case less sensitive to chlorine
732 emissions, producing less ClNO₂ and Cl atoms compared with the Base case (with Yu parameterization)
733 although with the same emission. ~~Consequently~~Consequently, the McDuffie case produces less O₃, with
734 annual mean surface concentrations of MDA8 O₃ lower by 0.47 ppbv averaged in China (by up to 2 ppbv
735 in the SCBSichuan Basin), but results in more PM_{2.5} (0.63 μg m⁻³ averaged in China and up to 4.7 μg m⁻³
736 in the SCBSichuan Basin on annual mean basis) mainly due to ~~changes in NO₃⁻~~ (Fig. 8). In other
737 words, compared to the Base case with ~~the~~ Yu parameterization, the impacts of chlorine emissions on
738 annual MDA8 O₃ and PM_{2.5} in the McDuffie case has been decreased by 48% and 27% ~~respectively~~
739 averaged in China, ~~respectively~~. Therefore, even with the same amounts of ~~chlorine~~ emissions, the
740 impacts of ~~the heterogeneous N₂O₅ + ClN₂O₅ → ClNO₂ chemistry on air quality vary~~ies significantly with
741 different parameterizations.

742 4 Conclusions

743 Considering the importance of chlorine chemistry in modulating the O₃ and PM_{2.5} as well as the
744 previously ignored chlorine emission from anthropogenic and biomass burning, we updated the GOES-
745 Chem model in this study with comprehensive chlorine emissions and a new parameterization based on
746 the study of Yu et al. (2020) for ~~the heterogeneous N₂O₅ + ClN₂O₅ → ClNO₂ chemistry~~, followed by the
747 extensive evaluation of model performance. Through the utilization of a large number of observational
748 datasets, we found a substantial improvement has been achieved by the additional chlorine emissions,
749 with NMB decreasing from -96% – -79% to -36% – 39% for Cl⁻ simulation. The comparison with
750 observed N₂O₅ and ClNO₂ also indicates better model performance with Yu parameterization while $\gamma_{\text{N}_2\text{O}_5}$
751 and ϕ_{ClNO_2} are underestimated in McDuffie parameterization (a default setting in GEOS-Chem), resulting
752 in larger model bias. The simulation of O₃ and PM_{2.5} also agrees better with observations in general in

带格式的: 字体: 倾斜

带格式的: 字体: 非倾斜

753 the Base case (with the additional chlorine emissions and Yu parameterization) than the others.

754 Total tropospheric chlorine chemistry could increase Cl atoms by up to $7 \times 10^3 \text{ molec cm}^{-3}$, and leads to
755 an increase of up to 4.5 ppbv in MDA8 O₃ but a decrease of up to $7.9 \mu\text{g m}^{-3}$ in PM_{2.5} concentrations on
756 an annual mean basis in China. The decrease in PM_{2.5} is mainly associated with the decrease in NO₃⁻ and
757 NH₄⁺, by up to 6.4 and $1.9 \mu\text{g m}^{-3}$, respectively. The results also indicate that the [heterogeneous N₂O₅ +](#)
758 [ClN₂O₅—ClNO₂](#) chemistry dominate the impact of chlorine chemistry, accounting for 83% and 90% of
759 total change in O₃ and PM_{2.5} concentrations. In other words, the chlorine chemistry without the
760 [heterogeneous N₂O₅ + ClN₂O₅—ClNO₂](#) chemistry has a minor effect on annual mean MDA8 O₃ (less
761 than 0.7 ppbv) and PM_{2.5} (less than $1.5 \mu\text{g m}^{-3}$) concentrations in China. This mechanism is particularly
762 useful in elucidating the commonly seen O₃ underestimations [relative to observations](#) (e.g. (Ma et al.
763 (2019))).

764 The effect of [the heterogeneous N₂O₅ + ClN₂O₅—ClNO₂](#) chemistry is sensitive to chlorine emissions. ←
765 With the additional anthropogenic and biomass burning sources, simulated PM_{2.5} concentrations are
766 increased by up to $4.5 \mu\text{g m}^{-3}$ in the [North China PlainNCP](#) but decreased by up to $3.7 \mu\text{g m}^{-3}$ in the
767 [SCBSichuan Basin](#) on an annual basis. The latter is mainly driven by the decrease of NO₃⁻ due to the
768 competition between the formation of ClNO₂ and HNO₃ upon the uptake of N₂O₅ on aerosol surfaces.
769 The additional emissions also increase Cl atoms and OH in China associated with the photolysis of
770 ClNO₂, consequently leading to an increase of annual mean MDA8 O₃ concentrations by up to 3.5 ppbv.
771 In contrast, the significance of the [heterogeneous N₂O₅ + ClN₂O₅—ClNO₂](#) chemistry especially over
772 inland China would be severely underestimated if only sea salt chlorine is considered, with only a slight
773 increase in MDA8 O₃ (< 0.5 ppbv) and a minor decrease in PM_{2.5} (< $1.5 \mu\text{g m}^{-3}$) in inland China.

774 Moreover, we found the importance of chlorine chemistry not only depends on the amount of emissions,
775 but is also sensitive to the parameterizations for [the heterogeneous N₂O₅ + ClN₂O₅—ClNO₂](#) chemistry.
776 Although with the same emission, the effects on MDA8 O₃ and PM_{2.5} in China from the McDuffie case
777 are lower compared to the results with ~~the~~ Yu parameterization: differing by 48% and 27% in the annual
778 average, respectively.

带格式的: 段落间距段后: 1 行

779 **Acknowledgements**

780 This study is supported by the National key R&D Program of China (2018YFC0213901), the National
781 Natural Science Foundation of China (41907182, 41877303, 91644218, 41877302, 41875156), the
782 Fundamental Research Funds for the Central Universities (21621105), Guangdong Natural Science
783 Funds for Distinguished Young Scholar (grant No. 2018B030306037), the Guangdong Innovative and
784 Entrepreneurial Research Team Program (Research team on atmospheric environmental roles and
785 effects of carbonaceous species: 2016ZT06N263), and Special Fund Project for Science and
786 Technology Innovation Strategy of Guangdong Province (2019B121205004).

787 **Competing interests.**

788 The authors declare that they have no conflict of interest.

789 **Data and Code availability**

790 ~~Both the~~ ~~The~~ data ~~and source code of the revised model~~ used in this study ~~are~~ ~~is~~ available upon request
791 from Qiaoqiao Wang (qwang@jnu.edu.cn). ~~The revised codes for different simulations could be~~
792 ~~downloaded via~~ <https://zenodo.org/record/5957287#.YfyNMppBxPZ>

793 **References**

794 Anttila, T., Kiendler-Scharr, A., Tillmann, R., and Mentel, T. F.: On the Reactive Uptake of Gaseous
795 Compounds by Organic-Coated Aqueous Aerosols: Theoretical Analysis and Application to the
796 Heterogeneous Hydrolysis of N₂O₅, *The Journal of Physical Chemistry A*, 110, 10435-10443,
797 10.1021/jp062403c, 2006.

798 Atkinson, R., Baulch, D. L., Cox, R. A., Crowley, J. N., Hampson, R. F., Hynes, R. G., Jenkin, M. E.,
799 Rossi, M. J., Troe, J., and Subcommittee, I.: Evaluated kinetic and photochemical data for
800 atmospheric chemistry: Volume II - gas phase reactions of organic species, *Atmos. Chem. Phys.*, 6,
801 3625-4055, 10.5194/acp-6-3625-2006, 2006.

802 Bertram, T. H. and Thornton, J. A.: Toward a general parameterization of N₂O₅ reactivity on aqueous
803 particles: the competing effects of particle liquid water, nitrate and chloride, *Atmospheric Chemistry
804 & Physics Discussions*, 9, 191-198, 2009.

805 Bertram, T. H., Perring, A. E., Wooldridge, P. J., Dibb, J., Avery, M. A., and Cohen, R. C.: On the export
806 of reactive nitrogen from Asia: NO_x partitioning and effects on ozone, *Atmos. Chem. Phys.*, 13,
807 4617-4630, 10.5194/acp-13-4617-2013, 2013.

808 Chang, W. L., Brown, S. S., Stutz, J., Middlebrook, A. M., Bahreini, R., Wagner, N. L., Dubé, W. P.,
809 Pollack, I. B., Ryerson, T. B., and Riemer, N.: Evaluating N₂O₅ heterogeneous hydrolysis
810 parameterizations for CalNex 2010, *J. Geophys. Res.: Atmos.*, 121, 5051-5070,
811 <https://doi.org/10.1002/2015JD024737>, 2016.

812 Chen, C., Zhang, H., Yan, W., Wu, N., Zhang, Q., and He, K.: Aerosol water content enhancement leads
813 to changes in the major formation mechanisms of nitrate and secondary organic aerosols in winter
814 over the North China Plain, *Environ. Pollut.*, 287, 117625,
815 <https://doi.org/10.1016/j.envpol.2021.117625>, 2021a.

816 Chen, W., Ye, Y., Hu, W., Zhou, H., Pan, T., Wang, Y., Song, W., Song, Q., Ye, C., Wang, C., Wang, B.,
817 Huang, S., Yuan, B., Zhu, M., Lian, X., Zhang, G., Bi, X., Jiang, F., Liu, J., Canonaco, F., Prevot,
818 A. S. H., Shao, M., and Wang, X.: Real-Time Characterization of Aerosol Compositions, Sources,
819 and Aging Processes in Guangzhou During PRIDE-GBA 2018 Campaign, *J. Geophys. Res.: Atmos.*,
820 126, e2021JD035114, <https://doi.org/10.1029/2021JD035114>, 2021b.

821 Choi, M. S., Qiu, X., Zhang, J., Wang, S., Li, X., Sun, Y., Chen, J., and Ying, Q.: Study of Secondary
822 Organic Aerosol Formation from Chlorine Radical-Initiated Oxidation of Volatile Organic
823 Compounds in a Polluted Atmosphere Using a 3D Chemical Transport Model, *Environ. Sci.
824 Technol.*, 54, 13409-13418, 10.1021/acs.est.0c02958, 2020.

825 Dai, J., Liu, Y., Wang, P., Fu, X., Xia, M., and Wang, T.: The impact of sea-salt chloride on ozone through
826 heterogeneous reaction with N₂O₅ in a coastal region of south China, *Atmos. Environ.*, 236, 117604,
827 <https://doi.org/10.1016/j.atmosenv.2020.117604>, 2020.

828 DeCarlo, P. F., Kimmel, J. R., Trimborn, A., Northway, M. J., Jayne, J. T., Aiken, A. C., Gonin, M., Fuhrer,
829 K., Horvath, T., Docherty, K. S., Worsnop, D. R., and Jimenez, J. L.: Field-Deployable, High-
830 Resolution, Time-of-Flight Aerosol Mass Spectrometer, *Anal. Chem.*, 78, 8281-8289,
831 10.1021/ac061249n, 2006.

832 Finlayson-Pitts, B. J., Ezell, M. J., and Pitts, J. N. J.: Formation of chemically active chlorine compounds
833 by reactions of atmospheric NaCl particles with gaseous N₂O₅ and ClONO₂, *Cheminform*, 20, 241-
834 244, 1989.

835 Fountoukis, C. and Nenes, A.: ISORROPIA II: a computationally efficient thermodynamic equilibrium
836 model for $K^+-Ca^{2+}-Mg^{2+}-NH_4^+-Na^+-SO_4^{2-}-NO_3^- -Cl^- -H_2O$ aerosols, *Atmos. Chem. Phys.*, 7, 4639-
837 4659, 10.5194/acp-7-4639-2007, 2007.

838 Fu, X., Wang, T., Wang, S., Zhang, L., Cai, S., Xing, J., and Hao, J.: Anthropogenic Emissions of
839 Hydrogen Chloride and Fine Particulate Chloride in China, *Environ. Sci. Technol.*, 52, 1644, 2018.

840 Geng, G., Zhang, Q., Martin, R. V., Van Donkelaar, A., Huo, H., Che, H., Lin, J., and He, K.: Estimating
841 long-term PM_{2.5} concentrations in China using satellite-based aerosol optical depth and a chemical
842 transport model, *Remote Sens. Environ.*, 166, 262-270, 2015.

843 [Griffiths, P. T., Badger, C. L., Cox, R. A., Folkers, M., Henk, H. H., and Mentel, T. F.: Reactive Uptake](#)
844 [of N₂O₅ by Aerosols Containing Dicarboxylic Acids. Effect of Particle Phase, Composition, and](#)
845 [Nitrate Content, *The Journal of Physical Chemistry A*, 113, 5082-5090, 10.1021/jp8096814, 2009.](#)

846 [Gross, S., Iannone, R., Xiao, S., and Bertram, A. K.: Reactive uptake studies of NO₃ and N₂O₅ on](#)
847 [alkenoic acid, alkanolate, and polyalcohol substrates to probe nighttime aerosol chemistry, *PCCP*,](#)
848 [11, 7792-7803, 10.1039/B904741G, 2009.](#)

849 Guenther, A., Karl, T., Harley, P., Wiedinmyer, C., Palmer, P. I., and Geron, C.: Estimates of global
850 terrestrial isoprene emissions using MEGAN (Model of Emissions of Gases and Aerosols from
851 Nature), *Atmos. Chem. Phys.*, 6, 3181-3210, 10.5194/acp-6-3181-2006, 2006.

852 Haskins, J. D., Lee, B. H., Lopez-Hilifiker, F. D., Peng, Q., Jaeglé, L., Reeves, J. M., Schroder, J. C.,
853 Campuzano-Jost, P., Fibiger, D., McDuffie, E. E., Jiménez, J. L., Brown, S. S., and Thornton, J. A.:
854 Observational Constraints on the Formation of Cl₂ From the Reactive Uptake of ClNO₂ on Aerosols
855 in the Polluted Marine Boundary Layer, *J. Geophys. Res.: Atmos.*, 124, 8851-8869,
856 <https://doi.org/10.1029/2019JD030627>, 2019.

857 Hong, Y., Liu, Y., Chen, X., Fan, Q., Chen, C., Chen, X., and Wang, M.: The role of anthropogenic
858 chlorine emission in surface ozone formation during different seasons over eastern China, *Sci. Total*
859 *Environ.*, 723, 137697, <https://doi.org/10.1016/j.scitotenv.2020.137697>, 2020.

860 Hossaini, R., Chipperfield, M. P., Saiz-Lopez, A., Fernandez, R., Monks, S., Feng, W., Brauer, P., and
861 von Glasow, R.: A global model of tropospheric chlorine chemistry: Organic versus inorganic
862 sources and impact on methane oxidation, *J. Geophys. Res.: Atmos.*, 121, 214,271-214,297,
863 <https://doi.org/10.1002/2016JD025756>, 2016.

864 Huang, Z., Zhong, Z., Sha, Q., Xu, Y., Zhang, Z., Wu, L., Wang, Y., Zhang, L., Cui, X., Tang, M., Shi,
865 B., Zheng, C., Li, Z., Hu, M., Bi, L., Zheng, J., and Yan, M.: An updated model-ready emission
866 inventory for Guangdong Province by incorporating big data and mapping onto multiple chemical
867 mechanisms, *Sci. Total Environ.*, 769, 144535, <https://doi.org/10.1016/j.scitotenv.2020.144535>,

868 2021.

869 Jaeglé, L., Quinn, P. K., Bates, T. S., Alexander, B., and Lin, J. T.: Global distribution of sea salt aerosols:
870 new constraints from in situ and remote sensing observations, *Atmos. Chem. Phys.*, 11, 3137-3157,
871 10.5194/acp-11-3137-2011, 2011.

872 Kercher, J. P., Riedel, T. P., and Thornton, J. A.: Chlorine activation by N₂O₅: simultaneous, in situ
873 detection of ClNO₂ and N₂O₅ by chemical ionization mass spectrometry, *Atmospheric*
874 *Measurement Techniques Discussions*, 2009.

875 Lawler, M. J., Sander, R., Carpenter, L. J., Lee, J. D., and Saltzman, E. S.: HOCl and Cl₂ observations
876 in marine air, *Atmos. Chem. Phys.*, 11, 8115-8144, 10.5194/acp-11-7617-2011, 2011.

877 Le Breton, M., Hallquist, Å. M., Pathak, R. K., Simpson, D., Wang, Y., Johansson, J., Zheng, J., Yang,
878 Y., Shang, D., Wang, H., Liu, Q., Chan, C., Wang, T., Bannan, T. J., Priestley, M., Percival, C. J.,
879 Shallcross, D. E., Lu, K., Guo, S., Hu, M., and Hallquist, M.: Chlorine oxidation of VOCs at a semi-
880 rural site in Beijing: Significant chlorine liberation from ClNO₂ and subsequent gas and particle
881 phase Cl-VOC production, *Atmos. Chem. Phys.*, 18, 13013-13030, 10.5194/acp-18-13013-2018,
882 2018.

883 ~~Lee, B. H., Lopez-Hilfiker, F. D., Schroder, J. C., Campuzano Jost, P., Jimenez, J. L., McDuffie, E. E.,~~
884 ~~Fibiger, D. L., Veres, P. R., Brown, S. S., Campos, T. L., Weinheimer, A. J., Flocke, F. F., Norris, G.,~~
885 ~~O'Mara, K., Green, J. R., Fiddler, M. N., Billign, S., Shah, V., Jaeglé, L., and Thornton, J. A.:~~
886 ~~Airborne Observations of Reactive Inorganic Chlorine and Bromine Species in the Exhaust of Coal-~~
887 ~~Fired Power Plants, *J. Geophys. Res.: Atmos.*, 123, 11,225-241,237,~~
888 ~~<https://doi.org/10.1029/2018JD029284>, 2018.~~

889 Li, G., Su, H., Ma, N., Tao, J., Kuang, Y., Wang, Q., Hong, J., Zhang, Y., Kuhn, U., Zhang, S., Pan, X.,
890 Lu, N., Tang, M., Zheng, G., Wang, Z., Gao, Y., Cheng, P., Xu, W., Zhou, G., Zhao, C., Yuan, B.,
891 Shao, M., Ding, A., Zhang, Q., Fu, P., Sun, Y., Pöschl, U., and Cheng, Y.: Multiphase chemistry
892 experiment in Fogs and Aerosols in the North China Plain (McFAN): integrated analysis and
893 intensive winter campaign 2018, *Faraday Discuss.*, 226, 207-222, 10.1039/D0FD00099J, 2021.

894 Li, K., Jacob, D. J., Liao, H., Shen, L., Zhang, Q., and Bates, K. H.: Anthropogenic drivers of 2013–2017
895 trends in summer surface ozone in China, *P. Natl. Acad. Sci.*, 116, 422-427,
896 10.1073/pnas.1812168116, 2019.

897 Li, M., Zhang, Q., Kurokawa, J. I., Woo, J. H., He, K., Lu, Z., Ohara, T., Song, Y., Streets, D. G.,
898 Carmichael, G. R., Cheng, Y., Hong, C., Huo, H., Jiang, X., Kang, S., Liu, F., Su, H., and Zheng,
899 B.: MIX: a mosaic Asian anthropogenic emission inventory under the international collaboration
900 framework of the MICS-Asia and HTAP, *Atmos. Chem. Phys.*, 17, 935-963, 10.5194/acp-17-935-
901 2017, 2017.

902 Li, Q., Zhang, L., Wang, T., Tham, Y. J., Ahmadov, R., Xue, L., Zhang, Q., and Zheng, J.: Impacts of
903 heterogeneous uptake of dinitrogen pentoxide and chlorine activation on ozone and reactive
904 nitrogen partitioning: improvement and application of the WRF-Chem model in southern China,
905 *Atmos. Chem. Phys.*, 16, 14875-14890, 10.5194/acp-16-14875-2016, 2016.

906 Liu, X., Qu, H., Huey, L. G., Wang, Y., Sjostedt, S., Zeng, L., Lu, K., Wu, Y., Hu, M., Shao, M., Zhu, T.,
907 and Zhang, Y.: High Levels of Daytime Molecular Chlorine and Nitryl Chloride at a Rural Site on
908 the North China Plain, *Environ. Sci. Technol.*, 51, 9588-9595, 10.1021/acs.est.7b03039, 2017.

909 Liu, Y., Fan, Q., Chen, X., Zhao, J., Ling, Z., Hong, Y., Li, W., Chen, X., Wang, M., and Wei, X.:
910 Modeling the impact of chlorine emissions from coal combustion and prescribed waste incineration
911 on tropospheric ozone formation in China, *Atmos. Chem. Phys.*, 18, 2709-2724, 10.5194/acp-18-
912 2709-2018, 2018.

913 Lobert, J. M., Keene, W. C., Logan, J. A., and Yevich, R.: Global chlorine emissions from biomass
914 burning: Reactive Chlorine Emissions Inventory, *J. Geophys. Res.: Atmos.*, 104, 8373-8389,
915 <https://doi.org/10.1029/1998JD100077>, 1999.

916 Ma, M., Gao, Y., Wang, Y., Zhang, S., Leung, L. R., Liu, C., Wang, S., Zhao, B., Chang, X., Su, H.,
917 Zhang, T., Sheng, L., Yao, X., and Gao, H.: Substantial ozone enhancement over the North China
918 Plain from increased biogenic emissions due to heat waves and land cover in summer 2017, *Atmos.*
919 *Chem. Phys.*, 19, 12195-12207, 10.5194/acp-19-12195-2019, 2019.

920 McDuffie, E. E., Fibiger, D. L., Dubé, W. P., Lopez-Hilfiker, F., Lee, B. H., Jaeglé, L., Guo, H., Weber,
921 R. J., Reeves, J. M., Weinheimer, A. J., Schroder, J. C., Campuzano-Jost, P., Jimenez, J. L., Dibb, J.
922 E., Veres, P., Ebben, C., Sparks, T. L., Wooldridge, P. J., Cohen, R. C., Campos, T., Hall, S. R.,
923 Ullmann, K., Roberts, J. M., Thornton, J. A., and Brown, S. S.: ClNO₂ Yields From Aircraft
924 Measurements During the 2015 WINTER Campaign and Critical Evaluation of the Current
925 Parameterization, *J. Geophys. Res.: Atmos.*, 123, 12,994-913,015,
926 <https://doi.org/10.1029/2018JD029358>, 2018a.

927 McDuffie, E. E., Fibiger, D. L., Dubé, W. P., Lopez-Hilfiker, F., Lee, B. H., Thornton, J. A., Shah, V.,
928 Jaeglé, L., Guo, H., Weber, R. J., Michael Reeves, J., Weinheimer, A. J., Schroder, J. C.,
929 Campuzano-Jost, P., Jimenez, J. L., Dibb, J. E., Veres, P., Ebben, C., Sparks, T. L., Wooldridge, P.
930 J., Cohen, R. C., Hornbrook, R. S., Apel, E. C., Campos, T., Hall, S. R., Ullmann, K., and Brown,
931 S. S.: Heterogeneous N₂O₅ Uptake During Winter: Aircraft Measurements During the 2015
932 WINTER Campaign and Critical Evaluation of Current Parameterizations, *J. Geophys. Res.: Atmos.*,
933 123, 4345-4372, <https://doi.org/10.1002/2018JD028336>, 2018b.

934 Mitroo, D., Gill, T. E., Haas, S., Pratt, K. A., and Gaston, C. J.: ClNO₂ Production from N₂O₅ Uptake
935 on Saline Playa Dusts: New Insights into Potential Inland Sources of ClNO₂, *Environ. Sci. Technol.*,

936 53, 7442-7452, 2019.

937 Morgan, W. T., Ouyang, B., Allan, J. D., Aruffo, E., Di Carlo, P., Kennedy, O. J., Lowe, D., Flynn, M. J.,
938 Rosenberg, P. D., Williams, P. I., Jones, R., McFiggans, G. B., and Coe, H.: Influence of aerosol
939 chemical composition on N₂O₅ uptake: airborne regional measurements in northwestern Europe,
940 *Atmos. Chem. Phys.*, 15, 973-990, 10.5194/acp-15-973-2015, 2015.

941 Ng, N. L., Herndon, S. C., Trimborn, A., Canagaratna, M. R., Croteau, P. L., Onasch, T. B., Sueper, D.,
942 Worsnop, D. R., Zhang, Q., Sun, Y. L., and Jayne, J. T.: An Aerosol Chemical Speciation Monitor
943 (ACSM) for Routine Monitoring of the Composition and Mass Concentrations of Ambient Aerosol,
944 *Aerosol Sci. Technol.*, 45, 780-794, 10.1080/02786826.2011.560211, 2011.

945 Osthoff, H. D., Roberts, J. M., Ravishankara, A. R., Williams, E. J., Lerner, B. M., Sommariva, R., Bates,
946 T. S., Coffman, D., Quinn, P. K., Dibb, J. E., Stark, H., Burkholder, J. B., Talukdar, R. K., Meagher,
947 J., Fehsenfeld, F. C., and Brown, S. S.: High levels of nitryl chloride in the polluted subtropical
948 marine boundary layer, *Nat. Geosci.*, 1, 324-328, 10.1038/ngeo177, 2008.

949 Riedel, T. P., Bertram, T. H., Crisp, T. A., Williams, E. J., Lerner, B. M., Vlasenko, A., Li, S. M., Gilman,
950 J., De Gouw, J., and Bon, D. M.: Nitryl Chloride and Molecular Chlorine in the Coastal Marine
951 Boundary Layer, *Environ. Sci. Technol.*, 46, 10463-10470, 2012.

952 Riemer, N., Vogel, H., Vogel, B., Anttila, T., Kiendler-Scharr, A., and Mentel, T. F.: Relative importance
953 of organic coatings for the heterogeneous hydrolysis of N₂O₅ during summer in Europe, *J. Geophys.*
954 *Res.: Atmos.*, 114, <https://doi.org/10.1029/2008JD011369>, 2009.

955 Saiz-Lopez, A. and von Glasow, R.: Reactive halogen chemistry in the troposphere, *Chem. Soc. Rev.*, 41,
956 6448-6472, 10.1039/C2CS35208G, 2012.

957 Sarwar, G., Simon, H., Xing, J., and Mathur, R.: Importance of tropospheric ClNO₂ chemistry across the
958 Northern Hemisphere, *Geophys. Res. Lett.*, 2014.

959 Schmidt, J. A., Jacob, D. J., Horowitz, H. M., Hu, L., Sherwen, T., Evans, M. J., Liang, Q., Suleiman, R.
960 M., Oram, D. E., Le Breton, M., Percival, C. J., Wang, S., Dix, B., and Volkamer, R.: Modeling the
961 observed tropospheric BrO background: Importance of multiphase chemistry and implications for
962 ozone, OH, and mercury, *J. Geophys. Res.: Atmos.*, 121, 11,819-811,835,
963 <https://doi.org/10.1002/2015JD024229>, 2016.

964 Sherwen, T., Evans, M. J., Sommariva, R., Hollis, L. D. J., Ball, S. M., Monks, P. S., Reed, C., Carpenter,
965 L. J., Lee, J. D., Forster, G., Bandy, B., Reeves, C. E., and Bloss, W. J.: Effects of halogens on
966 European air-quality, *Faraday Discuss.*, 200, 75-100, 10.1039/C7FD00026J, 2017.

967 Sherwen, T., Schmidt, J. A., Evans, M. J., Carpenter, L. J., Großmann, K., Eastham, S. D., Jacob, D. J.,
968 Dix, B., Koenig, T. K., Sinreich, R., Ortega, I., Volkamer, R., Saiz-Lopez, A., Prados-Roman, C.,

969 Mahajan, A. S., and Ordóñez, C.: Global impacts of tropospheric halogens (Cl, Br, I) on oxidants
970 and composition in GEOS-Chem, *Atmos. Chem. Phys.*, 16, 12239-12271, 10.5194/acp-16-12239-
971 2016, 2016.

972 Simmonds, P. G., Manning, A. J., Cunnold, D. M., McCulloch, A., O'Doherty, S., Derwent, R. G.,
973 Krummel, P. B., Fraser, P. J., Dunse, B., Porter, L. W., Wang, R. H. J., Grealley, B. R., Miller, B. R.,
974 Salameh, P., Weiss, R. F., and Prinn, R. G.: Global trends, seasonal cycles, and European emissions
975 of dichloromethane, trichloroethene, and tetrachloroethene from the AGAGE observations at Mace
976 Head, Ireland, and Cape Grim, Tasmania, *J. Geophys. Res.: Atmos.*, 111,
977 <https://doi.org/10.1029/2006JD007082>, 2006.

978 Simpson, W. R., Brown, S. S., Saiz-Lopez, A., Thornton, J. A., and von Glasow, R.: Tropospheric
979 Halogen Chemistry: Sources, Cycling, and Impacts, *Chem. Rev.*, 115, 4035-4062,
980 10.1021/cr5006638, 2015.

981 Staudt, S., Gord, J. R., Karimova, N. V., McDuffie, E. E., Brown, S. S., Gerber, R. B., Nathanson, G. M.,
982 and Bertram, T. H.: Sulfate and Carboxylate Suppress the Formation of ClNO₂ at Atmospheric
983 Interfaces, *ACS Earth and Space Chemistry*, 3, 1987-1997, 10.1021/acsearthspacechem.9b00177,
984 2019.

985 [Thornton, J. A., Braban, C. F., and Abbatt, J. P. D.: N₂O₅ hydrolysis on sub-micron organic aerosols: the
986 effect of relative humidity, particle phase, and particle size, *PCCP*, 5, 4593-4603, 10.1039/B307498F,
987 2003.](#)

988 Tian, M., Liu, Y., Yang, F., Zhang, L., Peng, C., Chen, Y., Shi, G., Wang, H., Luo, B., Jiang, C., Li, B.,
989 Takeda, N., and Koizumi, K.: Increasing importance of nitrate formation for heavy aerosol pollution
990 in two megacities in Sichuan Basin, southwest China, *Environ. Pollut.*, 250, 898-905,
991 <https://doi.org/10.1016/j.envpol.2019.04.098>, 2019.

992 Van, d. W., G. R., Randerson, J. T., Giglio, L., Collatz, G. J., Mu, M., Kasibhatla, P. S., Morton, D. C.,
993 Defries, R. S., Jin, Y., and Van Leeuwen, T. T.: Global fire emissions and the contribution of
994 deforestation, savanna, forest, agricultural, and peat fires (1997–2009), *Atmos. Chem. Phys.*, 10,
995 16153-16230, 10.5194/acp-10-11707-2010, 2010.

996 Wang, S., Su, H., Chen, C., Tao, W., Streets, D. G., Lu, Z., Zheng, B., Carmichael, G. R., Lelieveld, J.,
997 Pöschl, U., and Cheng, Y.: Natural gas shortages during the “coal-to-gas” transition in China have
998 caused a large redistribution of air pollution in winter 2017, *P. Natl. Acad. Sci.*, 117, 31018-31025,
999 10.1073/pnas.2007513117, 2020a.

1000 Wang, X., Jacob, D. J., Fu, X., Wang, T., and Liao, H.: Effects of Anthropogenic Chlorine on PM 2.5 and
1001 Ozone Air Quality in China, *Environ. Sci. Technol.*, 54, 9908-9916, 2020b.

1002 Wang, X., Jacob, D. J., Eastham, S. D., Sulprizio, M. P., Zhu, L., Chen, Q., Alexander, B., Sherwen, T.,
1003 Evans, M. J., Lee, B. H., Haskins, J. D., Lopez-Hilfiker, F. D., Thornton, J. A., Huey, G. L., and
1004 Liao, H.: The role of chlorine in global tropospheric chemistry, *Atmos. Chem. Phys.*, 19, 3981-4003,
1005 10.5194/acp-19-3981-2019, 2019.

1006 Wang, Y., Shen, L., Wu, S., Mickley, L., He, J., and Hao, J.: Sensitivity of surface ozone over China to
1007 2000–2050 global changes of climate and emissions, *Atmos. Environ.*, 75, 374-382, 2013.

1008 Xia, M., Wang, W., Wang, Z., Gao, J., Li, H., Liang, Y., Yu, C., Zhang, Y., Wang, P., Zhang, Y., Bi, F.,
1009 Cheng, X., and Wang, T.: Heterogeneous Uptake of N₂O₅ in Sand Dust and Urban Aerosols
1010 Observed during the Dry Season in Beijing, *Atmosphere*, 10, 204, 2019.

1011 Xu, Z., Liu, M., Zhang, M., Song, Y., Wang, S., Zhang, L., Xu, T., Wang, T., Yan, C., Zhou, T., Sun, Y.,
1012 Pan, Y., Hu, M., Zheng, M., and Zhu, T.: High efficiency of livestock ammonia emission controls
1013 in alleviating particulate nitrate during a severe winter haze episode in northern China, *Atmos. Chem.*
1014 *Phys.*, 19, 5605-5613, 10.5194/acp-19-5605-2019, 2019.

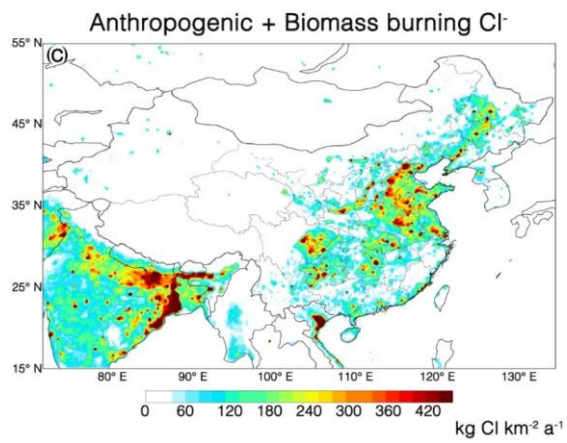
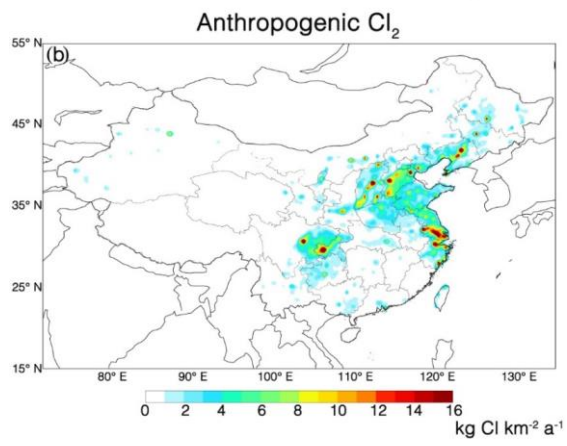
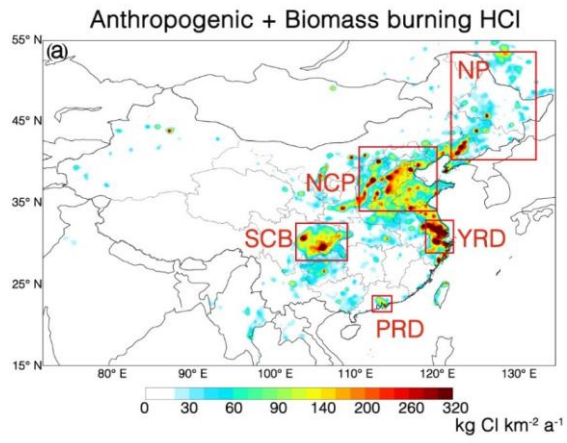
1015 Yang, X., Wang, T., Xia, M., Gao, X., Li, Q., Zhang, N., Gao, Y., Lee, S., Wang, X., Xue, L., Yang, L.,
1016 and Wang, W.: Abundance and origin of fine particulate chloride in continental China, *Sci. Total*
1017 *Environ.*, 624, 1041-1051, <https://doi.org/10.1016/j.scitotenv.2017.12.205>, 2018.

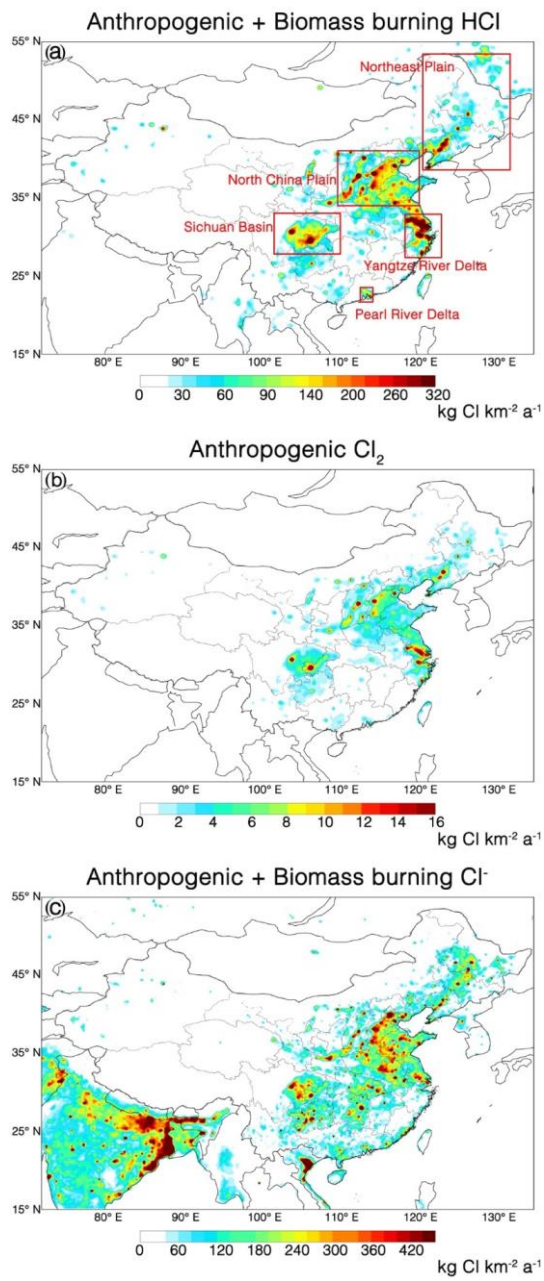
1018 Ye, C., Yuan, B., Lin, Y., Wang, Z., Hu, W., Li, T., Chen, W., Wu, C., Wang, C., Huang, S., Qi, J., Wang,
1019 B., Wang, C., Song, W., Wang, X., Zheng, E., Krechmer, J. E., Ye, P., Zhang, Z., Wang, X., Worsnop,
1020 D. R., and Shao, M.: Chemical characterization of oxygenated organic compounds in the gas phase
1021 and particle phase using iodide CIMS with FIGAERO in urban air, *Atmos. Chem. Phys.*, 21, 8455-
1022 8478, 10.5194/acp-21-8455-2021, 2021.

1023 Yu, C., Wang, Z., Xia, M., Fu, X., Wang, W., Tham, Y. J., Chen, T., Zheng, P., Li, H., Shan, Y., Wang, X.,
1024 Xue, L., Zhou, Y., Yue, D., Ou, Y., Gao, J., Lu, K., Brown, S. S., Zhang, Y., and Wang, T.:
1025 Heterogeneous N₂O₅ reactions on atmospheric aerosols at four Chinese sites: improving model
1026 representation of uptake parameters, *Atmos. Chem. Phys.*, 20, 4367-4378, 10.5194/acp-20-4367-
1027 2020, 2020.

1028 Zhang, T., de Jong, M. C., Wooster, M. J., Xu, W., and Wang, L.: Trends in eastern China agricultural
1029 fire emissions derived from a combination of geostationary (Himawari) and polar (VIIRS) orbiter
1030 fire radiative power products, *Atmos. Chem. Phys.*, 20, 10687-10705, 10.5194/acp-20-10687-2020,
1031 2020.

1032

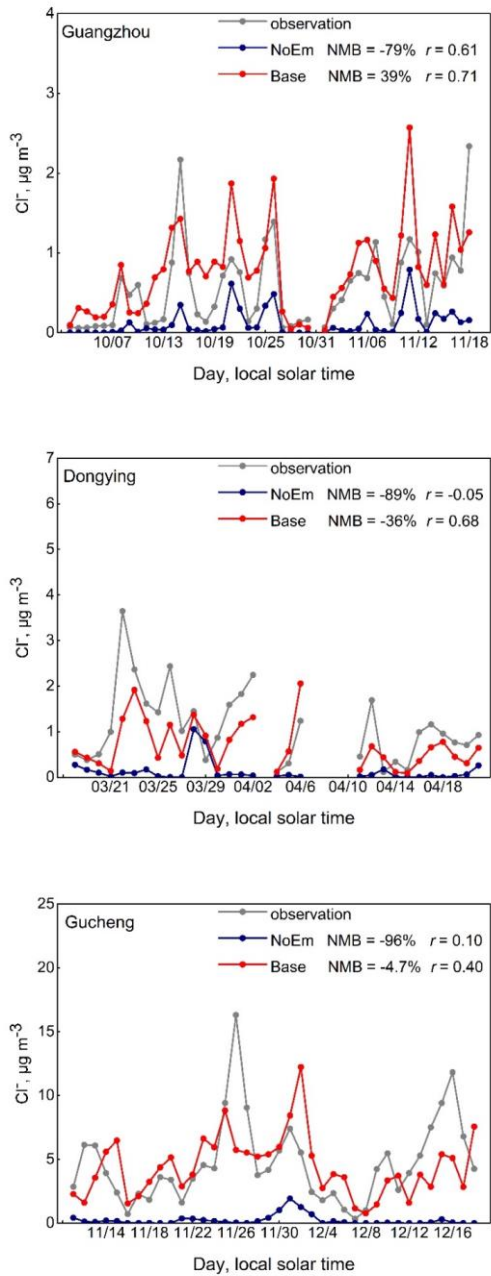




1034
1035
1036
1037

Figure 1. Annual emissions of (a) HCl, (b) Cl₂, (c) non-sea salt Cl⁻. Locations of the Northeast Plain, North China Plain, Yangtze River Delta, Pearl River Delta and Sichuan Basin are highlighted by red boxes in (a).

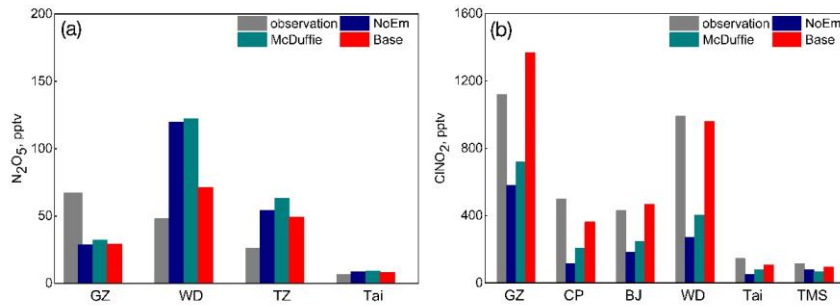
带格式的: 字体: 小五, 加粗



1038
1039
1040

Figure 2. Time series of simulated and observed particulate Cl^- concentrations at the Guangzhou, Dongying and Gucheng sites.

1041



1042

1043

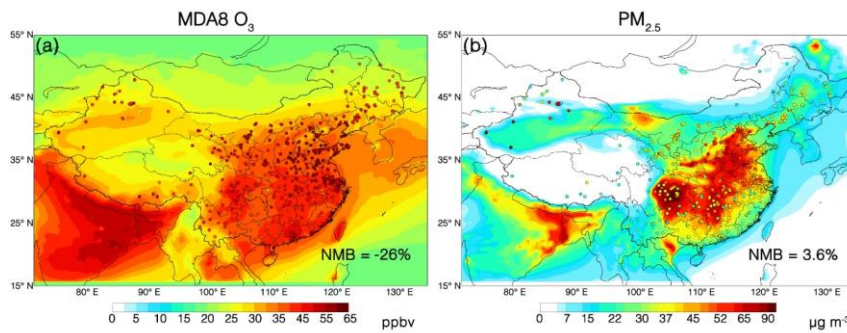
1044

1045

1046

1047

Figure 3. Comparison of observed and simulated (a) averaged N_2O_5 concentrations and (b) mean nighttime maximum mixing ratio of $ClNO_2$ concentrations at different sites. (The simulation definitions are provided in Table 2). GZ: Guangzhou; WD: Wangdu; TZ: Taizhou; Tai: Mount Tai; CP: Changping; BJ: Beijing; TMS: Mount TaiMoShan



1048

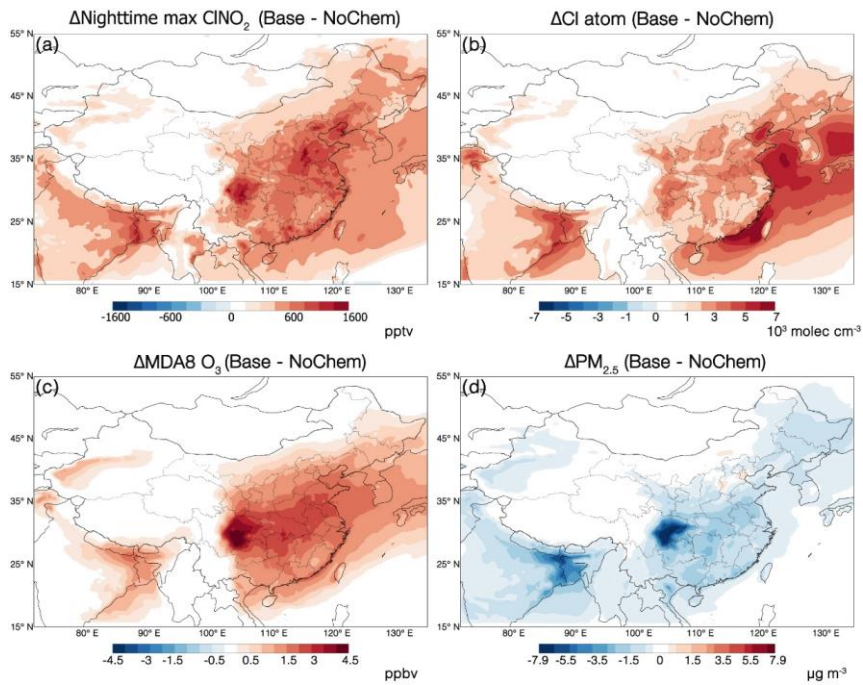
1049

1050

1051

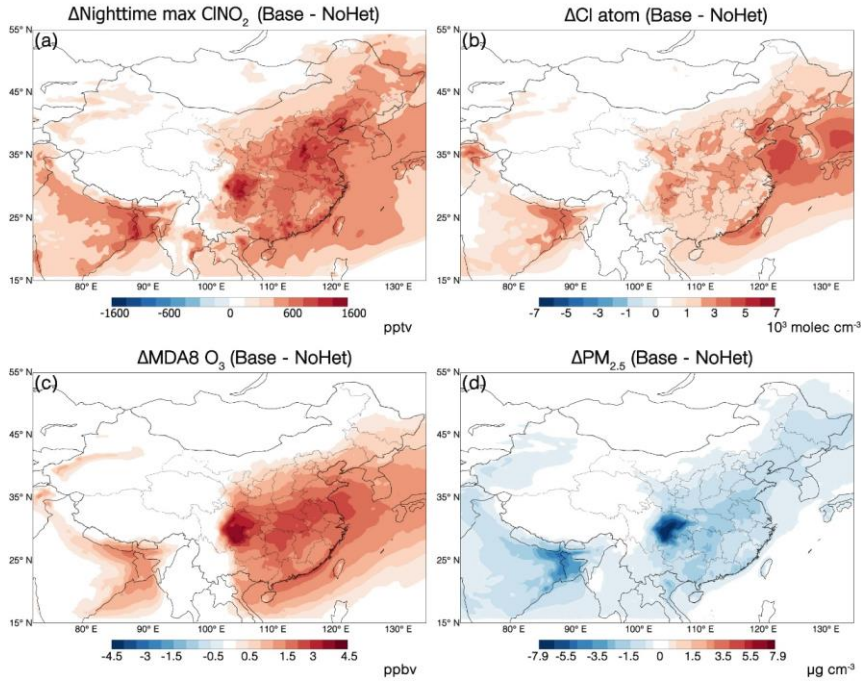
1052

Figure 4. Annual mean surface concentrations of (a) MDA8 O_3 and (b) $PM_{2.5}$ over China in 2018. GEOS-Chem model values from the Base case are shown as contours. Observations from China National Environmental Monitoring Center (CNEMC) are shown as circles.



1053
 1054
 1055
 1056
 1057

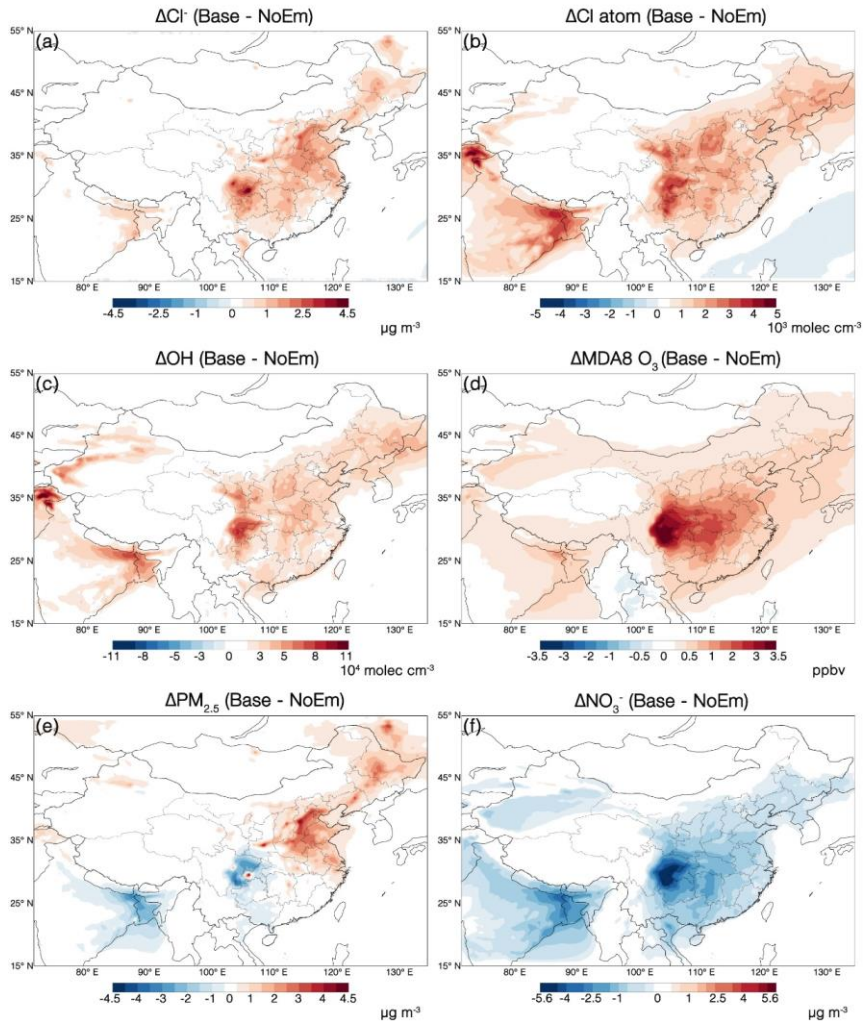
Figure 5. Effects of chlorine chemistry on annual mean surface concentrations of (a) nighttime max ClNO_2 , (b) Cl atom, (c) MDA8 O_3 and (d) $\text{PM}_{2.5}$ in China, estimated as the differences between the Base and NoChem cases.



1058
1059
1060
1061

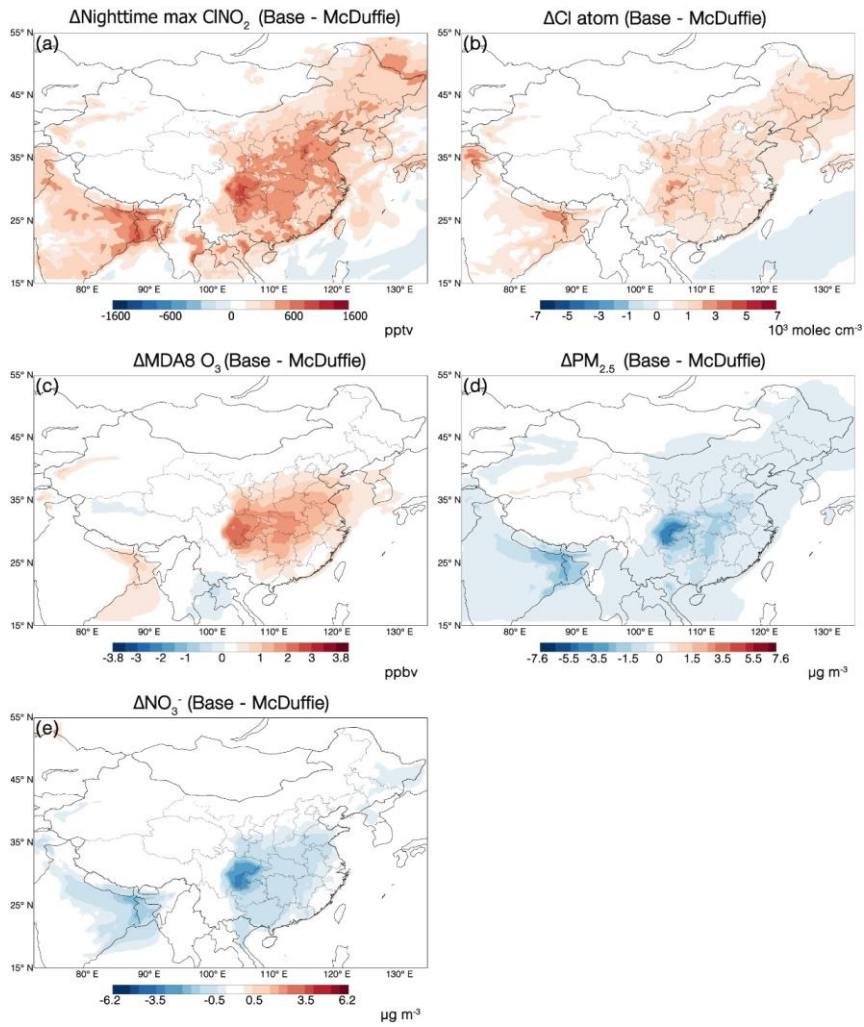
Figure 6. Effects of the heterogeneous N_2O_5 + Cl chemistry ~~N_2O_5 - ClNO_2 chemistry~~ on annual mean surface concentrations of (a) nighttime max ClNO_2 , (b) Cl atom, (c) MDA8 O_3 and (d) $\text{PM}_{2.5}$ in China, estimated as the differences between the Base and NoHet cases.

- 带格式的：字体：小五，加粗
- 带格式的：字体：小五，加粗，非上标/下标
- 带格式的：字体：小五，加粗
- 带格式的：非上标/下标
- 带格式的：非上标/下标
- 带格式的：非上标/下标



1062
 1063
 1064
 1065
 1066

Figure 7. Effects of anthropogenic and biomass burning chlorine emissions on annual mean surface concentrations of (a) Cl⁻, (b) Cl atom, (c) OH, (d) MDA8 O₃, (e) PM_{2.5} and (f) NO₃⁻ in China, estimated as the differences between the Base and NoEm cases.



1067
 1068 **Figure 8. Effects of different parameterizations on annual mean surface concentrations of (a) nighttime max**
 1069 **ClNO_2 , (b) Cl atom, (c) MDA8 O_3 , (d) $\text{PM}_{2.5}$, and (e) NO_3^- in China, estimated as the differences between the**
 1070 **Base and McDuffie cases.**

1071
 1072
 1073
 1074
 1075
 1076
 1077
 1078

1079

Table 1. Chlorine emissions in China in the model.

Sources	By default (Gg Cl a ⁻¹)	Updated in this study (Gg Cl a ⁻¹)
Sea salt Cl ⁻	6.5×10 ⁴	6.5×10 ⁴
Anthropogenic HCl	0	218
Biomass burning HCl	0	30
Anthropogenic Cl ₂	0	8.9
Anthropogenic Cl ⁻	0	379
Biomass burning Cl ⁻	0	120
CH ₃ Cl ^a	3.8	3.8
CH ₂ Cl ₂ ^a	2.4	2.4
CHCl ₃ ^a	0.70	0.70

1080 ^a: Sources are shown in terms of the chemical release (e.g. +Cl, +OH, +hv)

1081

1082

Table 2. Model setup of all simulation cases

Cases	N ₂ O ₅ uptake (γ _{N2O5})	ClNO ₂ production (φ _{ClNO2})	Other tropospheric chlorine chemistry	Anthropogenic and biomass burning inorganic chlorine emissions
Base	Yu et al. (2020)	Yu et al. (2020)	Full	Yes
McDuffie	McDuffie et al. (2018a, 2018b)	McDuffie et al. (2018a, 2018b)	Full	Yes
NoEm	Yu et al. (2020)	Yu et al. (2020)	Full	None
NoHet	Yu et al. (2020) but with [Cl ⁻] = 0	None	Full	Yes
NoChem	Yu et al. (2020) but with [Cl ⁻] = 0	None	None	Yes
NoEmHet	Yu et al. (2020) but with [Cl ⁻] = 0	None	Full	None
NoAll	Yu et al. (2020) but with [Cl ⁻] = 0	None	None	None

1083

1084

1085

Table 3. Normalized mean bias (NMB) and correlation coefficients (*r*) between observed and simulated MDA8 O₃ and PM_{2.5} concentrations during 2018 in China

Species	Time	Base		McDuffie		NoEm	
		NMB	<i>r</i>	NMB	<i>r</i>	NMB	<i>r</i>
MDA8 O ₃	Annual	-26%	0.83	-27%	0.83	-28%	0.82
	MAM ^a	-35%	0.87	-36%	0.87	-36%	0.87
	JJA ^b	-5.5%	0.50	-5.2%	0.48	-5.9%	0.48
	SON ^c	-24%	0.79	-26%	0.78	-28%	0.76
	DJF ^d	-49%	0.81	-53%	0.80	-54%	0.80
PM _{2.5}	Annual	3.6%	0.81	5.6%	0.81	2.3%	0.80
	MAM	-6.3%	0.52	-4.9%	0.53	-6.2%	0.52
	JJA	3.9%	0.70	4.6%	0.70	5.0%	0.70
	SON	28%	0.79	32%	0.80	26%	0.79
	DJF	-4.3%	0.82	-2.6%	0.82	-7.9%	0.82

1086 ^a: March, April, and May (Spring)1087 ^b: June, July, and August (Summer)1088 ^c: September, October, and November (Autumn)1089 ^d: December, January, and February (Winter)

1090